# DIAGNOSIS OF WATER PRODUCTION USING ARTIFICIAL NEURAL NETWORK MODELS

A thesis presented to the Department of Petroleum Engineering

African University of Science and Technology

In partial fulfilment of the requirements for the degree of

**MASTER OF SCIENCE IN PETROLEUM ENGINEERING**

By

**Ogunyemi, Samuel Shola**

Supervised by

Prof. David O. Ogbe

African University of Science and Technology
www.aust.edu.ng
P.M.B 681, Garki, Abuja F.C.T
Nigeria

**December, 2017**

## CERTIFICATION

This is to certify that the thesis titled "**DIAGNOSIS OF WATER PRODUCTION USING ARTIFICIAL NEURAL NETWORK MODELS**" submitted to the school of postgraduate studies, African University of Science and Technology (AUST), Abuja, Nigeria for the award of the Master's degree is a record of original research carried out by OGUNYEMI SAMUEL SHOLA in the Department of Petroleum Engineering.

DIAGNOSIS OF WATER PRODUCTION USING ARTIFICIAL NEURAL NETWORK MODELS

By

Ogunyemi, Samuel Shola

A THESIS APPROVED BY THE PETROLEUM ENGINEERING DEPARTMENT

**RECOMMENDED**: ……
**Supervisor**, Prof. David O. Ogbe

……
**Co-Supervisor**,

……
**Co-Supervisor**,

……
**Head**, Department of Petroleum Engineering

**APPROVED**: …….....
**Chief Academic Officer**

…….....
**Date**

**© 2017**
Ogunyemi, Samuel Shola

ALL RIGHTS RESERVED

## ABSTRACT

A data-driven approach to solving the problem of excess water production was the focus of this study. In this research, several reservoir models were simulated for 26 years, and data obtained after simulation was used to develop two artificial neural network models to predict the water cut for various producers. The first 22 years of data obtained from simulation was used to train the first neural network model, and the model was then used to forecast the water cut for the last four years of production. The developed neural network model was able to accurately forecast the water cut for the last four years of production of a well, with a regression coefficient of 0.9985 and mean square error of $1.5985*10^{-5}$. The second neural network model developed served a slightly different purpose. The model was developed to investigate its sensitivity to changes in reservoir conditions. Data used for training the second neural network model was obtained from the simulation results of a set of reservoir models, and the model was used for predicting well water cut of producers in a slightly modified version of those reservoir models. To investigate the sensitivity of the second model, the modified parameters included; permeability contrast, horizontal permeability, perforation interval of producers, the separation distance between an injector and a producer, and the initial aquifer pressure. The prediction by the second model was as good as the forecast by the first model and even better in some cases, indicating that the data-driven approach proposed in this work can serve as a technique for tackling the problem of excess water production in the oil and gas industry.



**Keyword:** Artificial neural network (ANN), Reservoir simulation, Water cut prediction, water production

## ACKNOWLEDGEMENT

The supervisory role of Prof. David O. Ogbe and his guidance toward the successful completion of this research cannot be overemphasized. Your contributions, positive criticism and time spent in bringing out the best in this work are immensely appreciated. Special thanks to Mr. Chuks Sunday, a student of Prof. David O. Ogbe, who took time to put me through the rudimentary aspect of the artificial neural network.

The support of my parents and siblings have been unbelievable and indescribable. Even though they made no direct intellectual contributions to this work, knowing fully well that I had supportive people around me, put in a state of mind where this research was carried out with ease and zero distraction.

I also acknowledge the Petroleum Technology Development Fund (PTDF) for offering me a scholarship and fully funding my program at AUST, I remain grateful. The energy, time and effort of the entire faculty and staff of the African University of Science and Technology are very much appreciated. For the gift of life and sound health, I will always be grateful to God.

## DEDICATION

This work is dedicated to everybody who has directly or indirectly contributed to its successful completion.

**TABLE OF CONTENT**

## LIST OF FIGURES

## LIST OF TABLES

# CHAPTER ONE

## 1.0 INTRODUCTION

### 1.1 Preamble

Water production is inevitable in the business of hydrocarbon production from an oil and gas reservoir, and this becomes much of a problem when the net profit is negatively impacted as a result of simultaneous water and hydrocarbon production. Excessive water production in mature fields is one of the major production challenges, and an estimated 50 billion dollars is gulped yearly to solve water production problems (Maurya *et al.,* 2014). Early water production is what every operator tries to avoid, which is most of the time achieved by optimum well placement. Optimum well placement requires a good understanding of the reservoir characteristics. However, an absolute understanding of the reservoir is impossible especially at the beginning of oil and gas production from the reservoir. So in most reservoirs, early water breakthrough followed by excessive water production is inevitable. Water also corrodes surface equipment, and the higher the volume of water produced, the more the corrosive tendency of the produced fluid, which further translates to an increased cost of operations.

The produced water could originate from the adjoining aquifer or injected water during secondary recovery processes. Depending on the well placement and the region of perforation, and the level of pressure depletion in the reservoir, water from the adjoined aquifer could cone into the producer well, especially in reservoirs with relatively high vertical permeability around the perforated intervals. Secondary recovery processes where the mobility of the injected fluid (water) is greater than that of the hydrocarbon (oil) in the reservoir result to fingering of the injection fluid through the reservoir fluid and eventual production of the injection fluid becomes inevitable. The flow of injection fluid through fractures, high thief zones, and high permeability

streaks could also promote the production of the injected water. Delaying water encroachment into the well is necessary as a way to manage the reservoir performance and to maximize the field's ultimate hydrocarbon recovery. It is of utmost importance to understand the mechanisms of water production to proffer solutions to this problem since water production resulting from different mechanisms requires different mitigation approaches (Al-Ghanim & Al-Nufaili, 2010).

Several techniques have been employed in the identification of excess water production mechanism. Ershaghi *et al.* did one of the earliest studies., in 1987. They applied the x-plot technique to the study water influx in the Sidi EI-Itayem reservoir in Tunisia. They were able to estimate water throughput at any water cut using field performance data. However, one major shortcoming of the x-plot is that it does not give any diagnostic information on the source of water production. Novotny (1995) applied the matrix flow evaluation technique for water control using production data and Darcy flow equation. Novotny based his diagnosis on the magnitude of the change in the calculated value of the absolute permeability of the formation using oil/water relative permeability values obtained from representative oil/water relative permeability relations for the reservoir. This type of diagnosis is highly dependent on the availability of reliable relative permeability data for the reservoir. Chan (1995) developed one of the most widely used methodologies for diagnosing the source of water influx. Chan used numerical simulations to study reservoir water conning and channelling, and observed that a log-log plot of water-oil ratio (WOR) and a derivative of WOR with respect to time (dWOR/dt) showed different trends for different water production mechanisms. Majid *et al.,* (2008) discussed the limitations of using production logging tools (PLT) to identify water inflow zones in highly deviated and horizontal wells. They further employed Chan's methodology in a horizontal well and obtained similar signatures similar to those obtained by Chan (1995).

Analytical and numerical study of water flooding under several conditions was done by Yortsos *et al.,* (1997). Chan's work motivated the study. They showed that the late time slope of Chan's diagnostic log-log plot could be related to the well pattern, the relative permeability characteristics or heterogeneity of the reservoir. These plots matched simulated results, but when applied to field cases, the effect of noise made it difficult to make good decisions (Egbe and Appah, 2005). Motivated by the work of Chan (1995) and Yortsos *et al.,* (1997), Egbe and Appah (2005) proposed a new methodology for diagnosing reservoir water production mechanism using time series analysis of water-oil ratio versus production time data. They applied their methodology to several field cases. They suggested that because the analyses of Chan (1995) and Yortsos *et al.,* (1997) were conducted in the time domain, the results were affected by noise. Egbe and Appah conducted their analyses in the frequency domain using power spectral analysis/Fourier transformation.

The use of artificial intelligence tools has gained some reputation over the years in the oil and gas industry. Artificial neural network (ANN) can work with noisy data and solve problems even if information related to detailed physics of the system of interest is not known, or the system too complex to be solved analytically (Nakutnyy *et al.,* 2008). Sunday (2016) applied artificial neural network to diagnose excess water production during oil and gas production, and he laid a foundation on which this study is built. This research focuses on the application of artificial neural network for diagnosis of excessive water production.

## 1.2 Problem Statement

Mitigation of excess water production requires proper understanding of the water production mechanisms, and the subsurface nature of a reservoir makes the accurate detection of the source

of water produced a difficult task. The methodologies employed by Chan (1995) and Yortsos *et al.,* (1997) are to date some of the best techniques for diagnosing the possible source or origin of produced water. However, they are still affected by noise and make decision making difficult (Egbe and Appah, 2005). Seright (1998) showed the limitations of Chan's plot and discouraged its use as a standalone tool for the identification of excess water production mechanisms. The results of Rabiei (2011) research buttressed Seright's claim. The literature shows the need to develop another approach to diagnose the mechanisms and solve the problem of excess water production in oil and gas reservoirs.

## 1.3 Aim and Objectives

**Aim**:

The research work aims at the application of artificial neural network to diagnose the problem of excess water production in oil and gas reservoirs.

**Objectives**:

The following objectives will achieve the aim of this research work

i. Development of robust artificial neural network models that can forecast well water cut over the useful life of the field. The robust neural network models must be capable of predicting water cut considering changes in reservoir properties and well configurations.
ii. Use of simulated field data for validation of the ANN models to determine their predictive accuracy and limitations.

## 1.4 Justification

This research work is justified by the following:

i. Present solutions to the problem of excess water production gulp an estimated $50 billion US dollars annually worldwide, justifying the need for research in other economically viable options for solving excessive water production problems.
ii. Chan's methods and its derivative methods are still affected by noise when applied to field cases, justifying the need for approaches that require little or no knowledge of the mechanism or source of excess water produced.
iii. Artificial neural networks can approximate relationships between variables controlling reservoir behaviour without understanding the exact mechanisms or detailed physics involved; this makes the simulation of reservoir behaviour and its response to changes in recovery parameters possible using ANN models.

## 1.5 Scope

The scope of this research is limited to the study of the water production profiles of a reservoir described in this work. It considers evolution of the water production arising from various changes in the reservoir characteristics and well configurations. The reservoir will be simulated using the Eclipse Reservoir Simulator to obtain production data, followed by the development of artificial neural network models to predict water cut.

# CHAPTER TWO

## 2.0 LITERATURE REVIEW

### 2.1 Excess Water Production Mechanism

Connate water is present in every reservoir, and in that regard, water is produced along with hydrocarbons during the recovery process. Produced water can be categorized into sweep, good, and bad water. The presence of water in or around the reservoir is not necessarily bad news; this is because water is a natural source of energy for pressure maintenance in a reservoir dominated by water drive. An active aquifer helps maintain reservoir pressure by moving water into the reservoir and occupying pore spaces that were previously occupied by produced hydrocarbons. In a situation where the aquifer strength weakens, water (sweep water) is injected into the reservoir to help maintain pressure. As the field approaches maturity, hydrocarbons are unavoidably produced along with the sweep water to maintain oil production rate. Water shutoff treatment remains unnecessary if the water-oil ratio (WOR) is below the economic limit (good water).

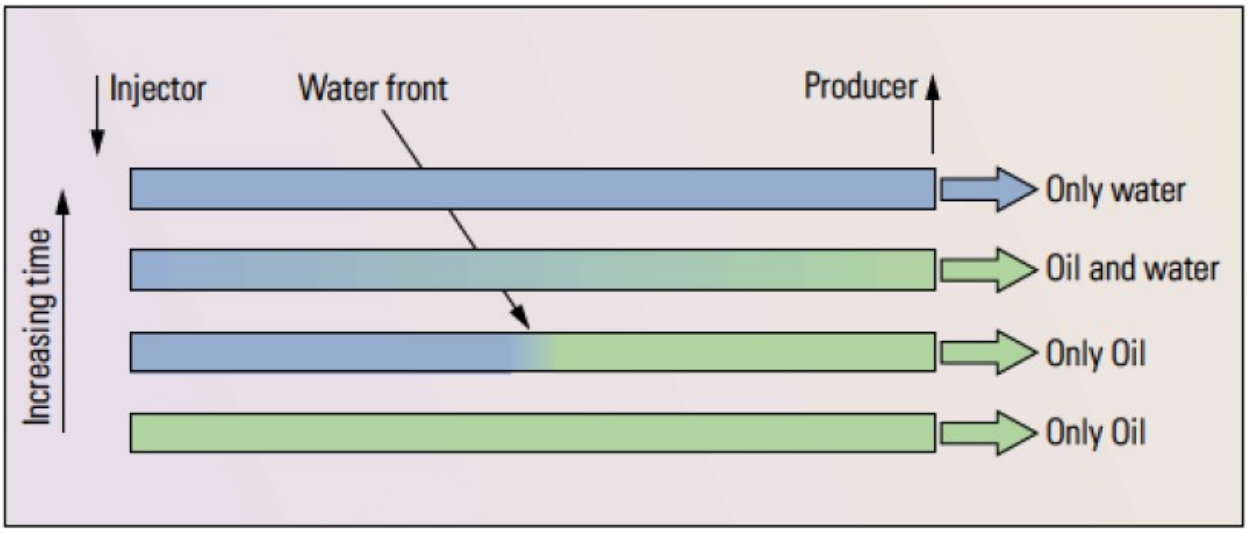


**Fig 2.1:** Advancing waterfront from an injector to a producer (Bailey *et al*., 2000).

Problems may, however, arise when water production exceeds the WOR economic limit, or when water from the aquifer or the injection water prematurely finds its way into the wellbore (bad water) (Bailey *et al*., 2000; Reynolds, 2003).

Excessive water production during the early stages of production decreases the volume of hydrocarbons that flow into the wellbore, increases the corrosive tendency of surface equipment and facilities, and further raises operating expense. During waterflood operation, early production of the injected water is an indication of high permeability intervals or channels that lead to reduced sweep efficiency.

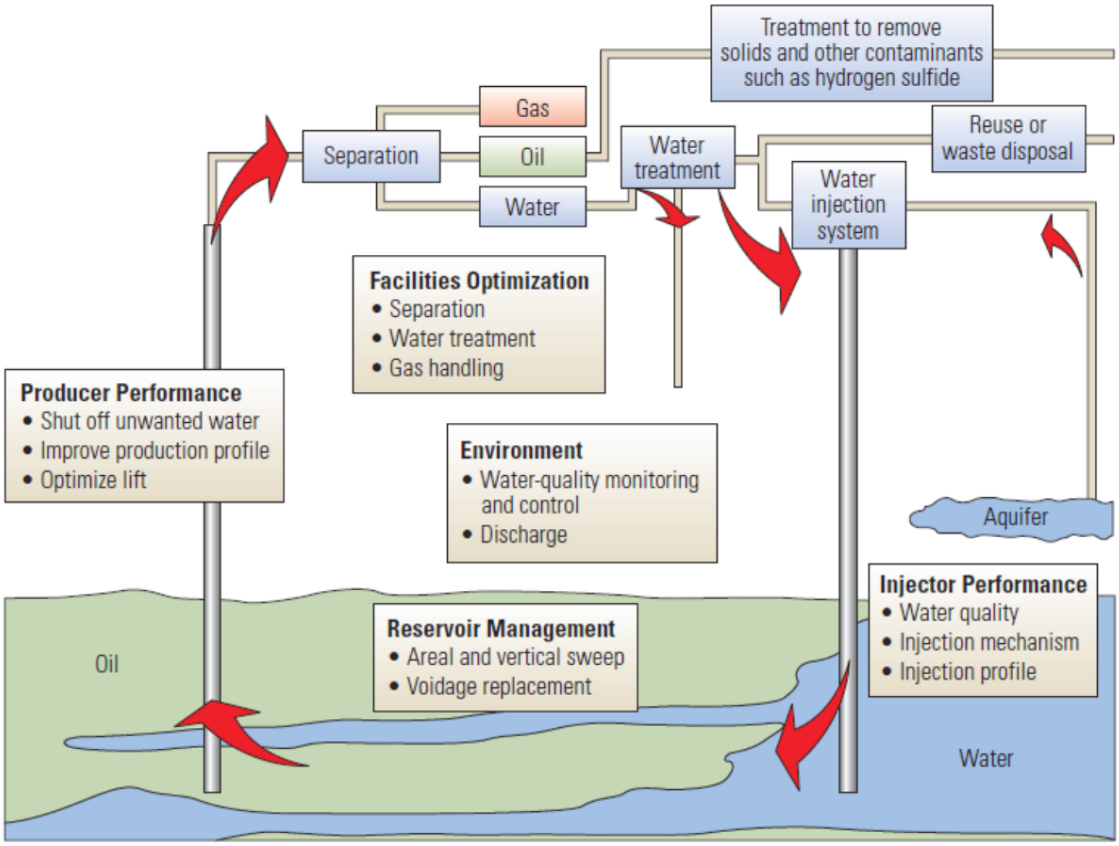


**Fig 2.2:** The oil and gas industry water management system (Arnold *et al*., 2004)

Water breakthrough increases water saturation around the wellbore and reduces the relative permeability of oil and gas. Excessive water production increases the fluid column head because

of a denser fluid being the larger fraction of the fluid mixture flowing through the wellbore. This brings about unnecessary expenses of lifting water to the surface and increased cost of water treatment facilities and water disposal systems. Figure 2.2 shows a schematic of a typical water management system used in the oil and industry.

A proper understanding of the mechanism of excess water production is required to mitigate this unfavourable situation in oil and gas operations. The mechanisms of water production can be classified using different criteria. Seright *et al.,* (2003) classified water production problems in terms of the difficulty of treatment (Table 2.1); the order of treatment difficulty increases from category A to D.

**Table 2.1:** Excess water production problems and treatment categories (Seright *et al*., 2003)

| **Category A: "Conventional" treatments** |
|---|
| • Casing leaks without flow restrictions |
| • Flow behind pipe without flow restrictions |
| • Non-fractured wells (injector or producers) with effective barriers to crossflow |
| **Category B: Treatment with Gelants** |
| • Casing leaks with flow restrictions |
| • Flow behind pipe with flow restrictions |
| • "2D coning" through a hydraulic fracture from an aquifer |
| • Natural fracture system leading to an aquifer |
| **Category C: Treatment with preformed Gels** |
| • Faults or fractures crossing a deviated or horizontal well |
| • Single fracture causing channelling between wells |
| • Natural fracture system allowing channelling between wells |
| **Category D: Difficult problems for which Gel treatments should not be used** |
| • 3D coning |
| • Cusping |
| • Channelling through strata (no fractures), with crossflow |

Bailey *et al.,* (2000), also classified water production mechanism into 10 basic types based on the ease of solving the problem. Reynolds and Kiker (2003) broadly categorised water production

problems into mechanical and communication problems. The classification by Bailey *et al.,* (2000) is adopted in this work.

### 2.1.1 Casing, Tubing and Packer leaks

Water from non-oil producing zones may flow into the wellbore if there is a leak in the casing, tubing or packer. Excessive formation pressure can cause collapse of the casing as well as excessive hydrostatic pressure leading to burst of the casing. Casing leak may also result from corrosion (Fig 2.3-A). Water flow logs or multiphase fluid logging tools can be used to identify possible locations where the leaks occur. Solution to this problem includes squeezing shutoff fluids and mechanical shutoff using plugs, cement and packers; patches can also be used.

### 2.1.2 Channel flow behind casing

Water-bearing zones can be connected to the pay zone because of failed primary cementing (Figure 2.3-B). Creation of voids behind the casing because of sand production can also be a secondary source of channels behind the casing. Channels behind casing can occur at any time during the production cycle but are most likely to occur immediately after well completion or stimulation. Temperature logs can be used to detect this problem, and the main solution is the use of shutoff fluids including high strength squeeze cement, resin-based fluid in the annulus, or lower strength gel-based fluids injected into the formation to prevent flow into the annulus.

### 2.1.3 Moving oil-water contact

Unwanted water production may also arise from a uniform bottom water contact moving toward the perforated zones in a well during normal water driven production (Figure 2.3-C). The chance

of having this kind of situation is much higher in reservoirs with low vertical permeability as compared to the reservoirs with higher vertical permeability where conning is much likely to occur.

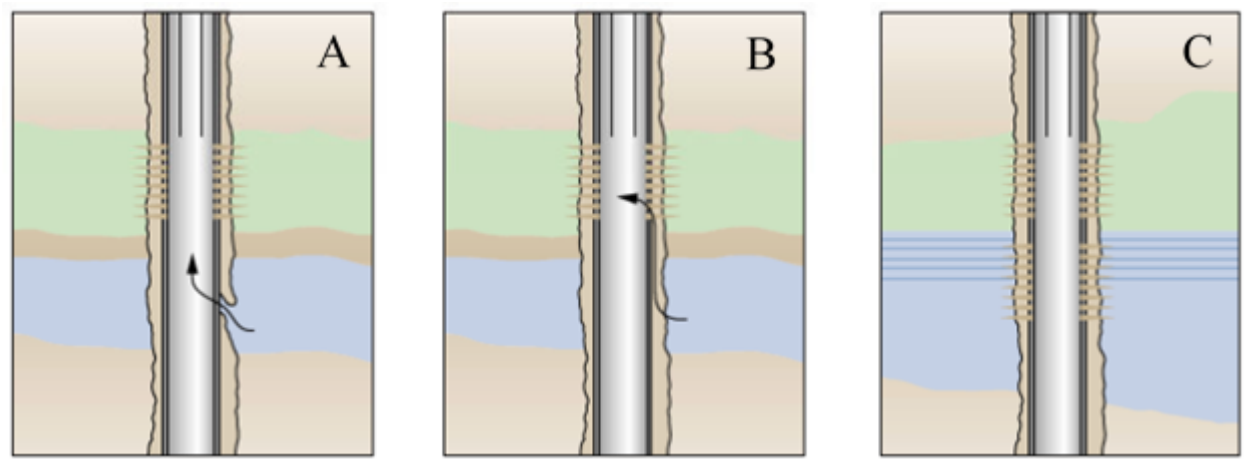


**Fig 2.3:** Casing, tubing or packer leaks (A), flow behind casing (B), and moving oil-water contact (Bailey *et al*., 2000).

### 2.1.4 Watered-out layer without cross flow

Production from a multilayer reservoir with barriers such as shale breaks below and above a high permeability zone will water out if the layer is in communication with an aquifer or flood water (Fig 2.4-A). This problem is easily solved in the absence of crossflow by application of rigid shutoff fluid or mechanical shutoff of the injector or producer well. This problem is not likely to occur in horizontal wells since they are completed mostly in one layer.

### 2.1.5 Watered-out layer with cross flow

Multilayer reservoirs that are not isolated by impermeable barriers are likely to experience water crossflow in zones with disparities in permeability (Figure 2.4-B). Like the case without crossflow, the highly permeable layer also waters out, but the vertical communication between

layers make treatment of the case with crossflow difficult. Shutoff of the highly permeable zone around the injector or producer become abortive since the flow can easily head in the vertical direction to other layers. Successful treatment in the case with crossflow is less likely; however if the economics is right, a deep penetrating gel can be injected into the thief zone.

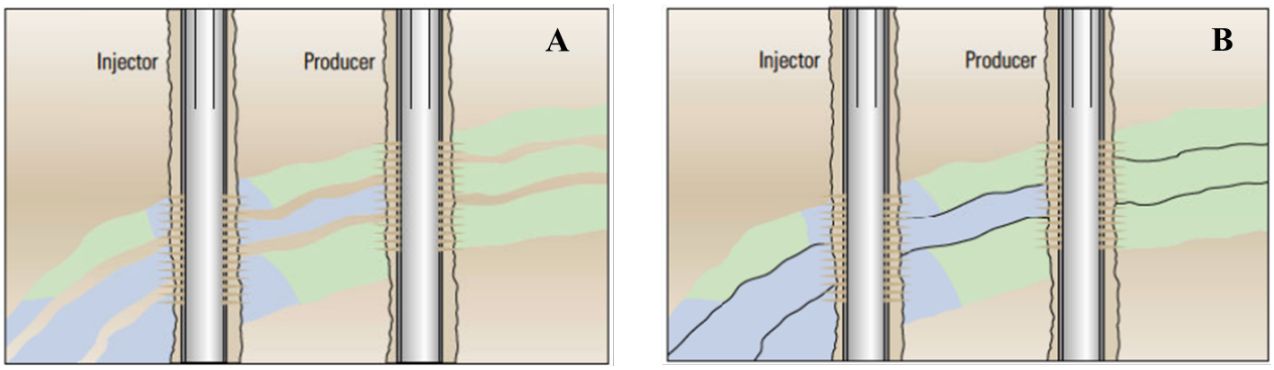


**Fig 2.4:** Watered out layer with crossflow (A) and without crossflow (B) (Bailey *et al*., 2000).

### 2.1.6 Fracture or faults between injector and producer

During waterflood operation in a naturally fractured reservoir, the breakthrough of injection water is imminent depending on the extensiveness of the reservoir fracture system (Figure 2.5-A). Pressure transient tests and inter-well tracers can be used to detect the presence of a considerable fracture system between the injector and producer. Injection of a flowing gel can mitigate excess water production without adversely affecting oil production from the formation.

### 2.1.7 Fracture or faults from a water layer

Fractures or faults intersecting a deeper water zone can lead to water production (Figure 2.5-B). Flowing gels can be used to address this kind of situation, especially when the fractures do not contribute to oil production. The appropriate volume of treatment gel is required, which is most of the time difficult to determine. The treatment gel is applied in such a way that fractures

contributing to oil flow are avoided, and it must be carefully tailored to resist flowback after the treatment operation. Fractures in most carbonate reservoirs are usually steep and tend to occur in clusters that are largely spaced from each other. Thus, there is a minimal chance of these fractures intersecting a vertical wellbore. This, however, is not the case for horizontal wells where water production is usually through fractures or faults that intersect the aquifer (Figure 2.5-C).

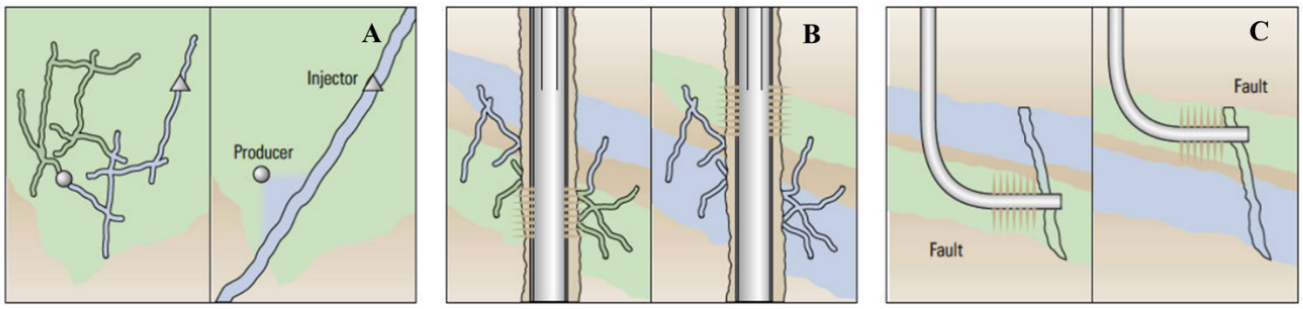


**Fig 2.5:** Fracture or faults between injector and producer (A), fracture or faults from water layer (B), and aquifer intersecting faults in horizontal well (C) (Bailey *et al*., 2000).

### 2.1.8 Coning or cusping

Coning occurs in formations with relatively high vertical permeability and in situations where a vertical well is perforated close to the water-oil contact, WOC (Figure 2.6-A). More often, the critical coning rate, which is the maximum rate at which oil can be produced without experiencing coning, is economically unsustainable. Gel placement above the equilibrium WOC could reduce coning rate but can rarely stop coning, since a large volume of gel is required for the operation which may not make economic sense, coupled with the difficulty in getting the gel deep into the formation. Re-perforation close to the top of the formation could solve the problem of coning if the earlier perforation was close to the GOC. Coning in a horizontal well is referred to as duning or cusping, which can be mitigated by near wellbore shutoff.

### 2.1.9 Poor areal sweep

Areal permeability anisotropy which is more severe in sand channel deposits can result to poor areal sweep, as well as injection during waterflooding or edge water from an aquifer (Figure 2.6-B). This problem of poor areal sweep is solved by diverting injected water away from the pore spaces which have already been swept by water, requiring continuous viscous flood or large treatment volume, both of which are not economic. Infill drilling will do a better job in proving recovery as well as lateral drain holes.

### 2.1.10 Gravity-segregated layer

Thick reservoirs with good vertical permeability can experience water production as a result of gravity segregation. Water from an aquifer or injection water flows downwards because it is heavier compared to the density of hydrocarbons and the minimal vertical resistance from the formation and only sweeps the lower portion of the reservoir (Figure 2.6-C). Formations with grains that become finer upwards as well as unfavourable oil-water mobility ratios worsen this problem. Shutting the lower perforation will temporarily solve the problem as gravity segregation will eventually dominate.

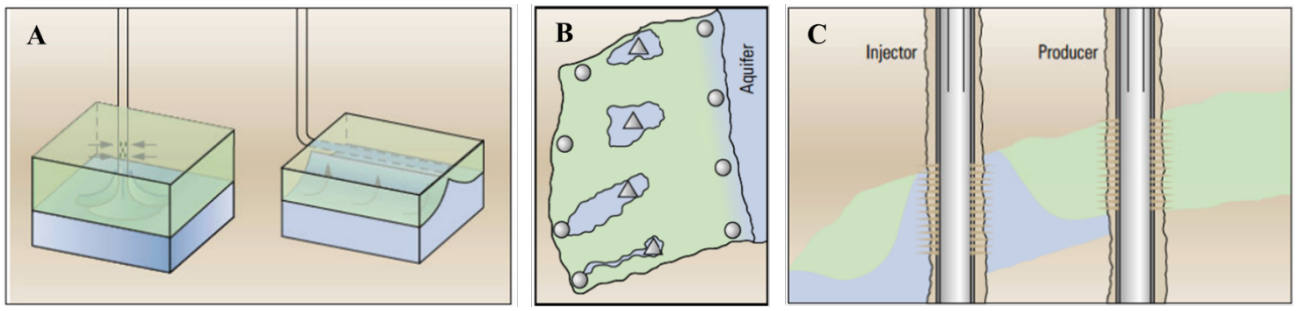


**Fig 2.6:** Coning or cusping (A), Poor areal sweep (B), and Gravity-segregated layer (C) (Bailey *et al*., 2000).

## 2.2 Conventional tool and techniques for well diagnostics and water control

Diagnosis and control of excess water production were trivialised in times past and thought of as simply a plug and cement, or gel treatment operation (Bailey *et al.,* 2000). Lack of understanding of the excess water production mechanisms and the subsequent application of wrong solution techniques was the reason behind the inability of the industry to control excess water production. It is therefore imperative to identify the mechanisms of excess water production in order to proffer effective and lasting solutions. Solution techniques are classified as mechanical (packers, plugs, and sleeves), chemical (foams, gel, cement, polymer, resins, and emulsion), and completion solutions (dual completion, multilateral wells and sidetracks). The efficiency of these techniques depends on the mechanism of water production (Reynolds, 2003). Well diagnostics is used to determine the existence of excess water production, locating the point of water entry in the well, and identifying the wells that require treatment (Bailey, 2000). Well diagnostic tools and techniques for identification of excess water production mechanisms can be categorised into two groups. One group includes logging and survey tools; the other group includes analytical and empirical techniques based on production data. This review focuses on the analytical and empirical techniques.

Reliable production history is required to employ these techniques. Production history contains lots of information that can help in the diagnosis of water production problem; the information includes oil and water production as well as the WOR. Several analytical techniques using the production history have been developed, they include recovery plot, decline curve analysis, production history plots among others.

### 2.2.1 Recovery plot

The recovery plot is a semilog plot of WOR against cumulative oil production (Figure 2.7). At any time, the recovery plot can be extrapolated to predict cumulative oil that will be produced at WOR economic limit. Based on the information obtained from the recovery plot, necessary water control action could be employed. (Bailey *et al.,* 2000).

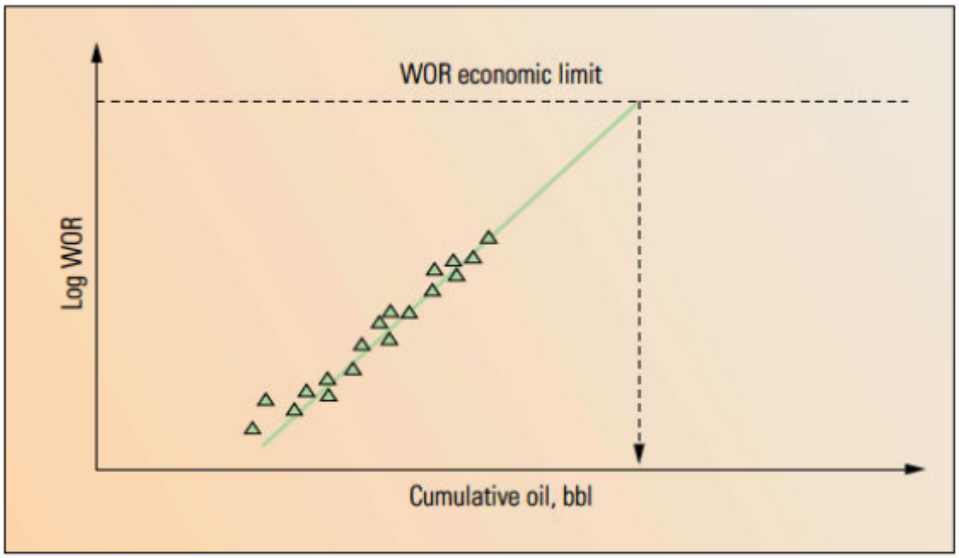


**Fig 2.7:** Recovery plot (Bailey *et al.,* 2000)

### 2.2.2 Production history plot

This is a log-log plot of oil and water production rate against time (Figure 2.8). Visualization of the rate of change during the life cycle of the field is made possible by this plot, "uncorrelated behaviour" such as rate change without corresponding pressure is elucidated by this plot (Rabiei, 2011). Wells requiring water control usually show a decreased oil production and an increased water production starting about the same time (Bailey *et al.,* 2000).

### 2.2.3 Decline curve analysis

Decline curve analysis is based on the theory that factors that determine past production will determine future production, hence production trend can be extrapolated to determine future production. A decline curve is usually a plot of production rate against time or cumulative

production of a well or an entire field (Figure 2.9). A linear decline is an indication of normal depletion, and any deviation for that straight line is an indication of a problem which may not be excess water production, but damage build-up or pressure depletion (Bailey *et al.,* 2000).

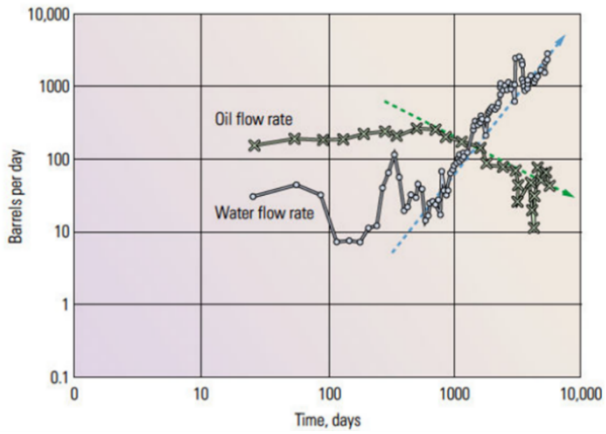


**Fig 2.8:** Production history plot (Bailey *et al.,* 2000)

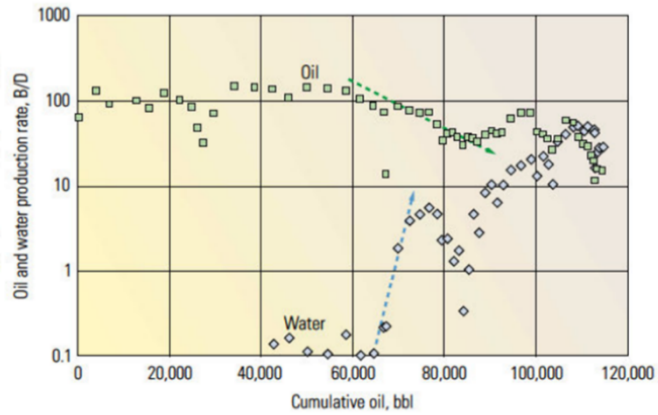


**Fig 2.9:** Decline curve (Bailey *et al.,* 2000)

### 2.2.4 Shut-in and choke-back analysis

According to Bailey *et al.,* (2000), production history containing periods of choke-back and shut-in, and analysis of the fluctuating water-oil ratio (WOR) could indicate the problem type. They stated that a decreased WOR during choke-back or after shut-in is an indication of a water entry problem such as coning or a single fracture intersecting a deeper water layer. On the contrary, WOR increases when the fracture or faults intersects an overlying water layer or when the water source is at a higher pressure than the oil zone.

### 2.2.5 NODAL analysis

Depending on the location temperature and pressure, fluid property changes during flow from the reservoir to the surface. The total pressure loss from the reservoir to the surface facility is because of resistance during fluid flow. The entire system can be broken into discrete nodes to analyse this pressure drop at each node in a process called NODAL analysis. Nodal analysis is

based on the principle of continuity. In other words, there exists only a unique pressure value at every node regardless of the location at that node (Boyun *et al.,* 2007).

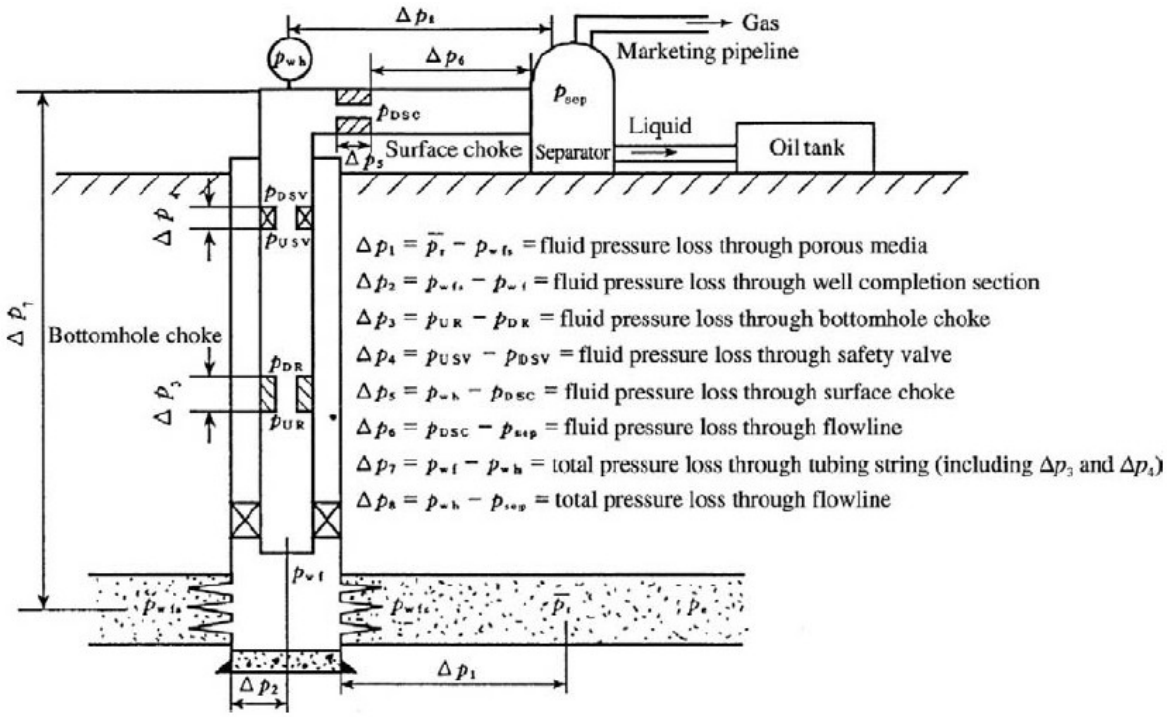


**Fig 2.10:** Pressure losses at various nodes in the production system (Renpu, 2011)

There are four nodes where this analysis takes place: pressure loss through porous media, pressure loss through well completion section, total pressure loss through the tubing string, and total pressure loss through flowlines (Renpu, 2011).

The pressure-rate relationship is known as the performance curve. The intersection between the inflow and outflow performance curves defines the operation point at the specified node. Although the NODAL analysis is mainly used to model wellbore responses, Bailey *et al.,* (2000) suggested its employability in the detection of excess water production mechanism.

### 2.2.6 Diagnostic Plots

Chan (1995) used a black oil simulator to conduct a series of water control numerical simulation, and he was able to generate a set of diagnostic plots. He was able to identify the mechanism of excess water production by making a log-log plot of WOR and its derivative against time (Chan's plot). In Chan's plot of WOR vs time (Figure 2.11), water channelling and coning showed different signatures, and three periods of WOR development could be identified. At the early stages of production, WOR curves remain flat, but as premature water breakthrough occur, deviation from this flat trend was observed. The time taken from the start of production to the start of this deviation is known as the departure time, which is shorter for coning as compared to channelling. The time when the bottom water cone hits the bottom of the perforation interval is the water coning departure time, while it is referred to as the water breakthrough time at any layer in a multilayer formation. A comprehensive description as to the proper identification of the water production mechanism is contained in Chan's study (1995). It is imperative to point out that Chan's methodology employs the WOR derivative plot in the identification of the excess water production mechanisms.

The work by Chan (1995) motivated the likes of Egbe and Appah (2005), and Yortsos *et al.,* (1997) to carry out further research to understand and improve on Chan's methodology. Egbe and Appah (2005) employed time series analysis of water-oil ratios using production field data, and they proposed a new methodology for diagnosing water production mechanisms. Egbe and Appah (2005) stated that the reason for the noise effect on Chan's plot was that the analysis was conducted in the time domain. They conducted their analysis in the frequency domain using power spectral analysis/Fourier transformation.

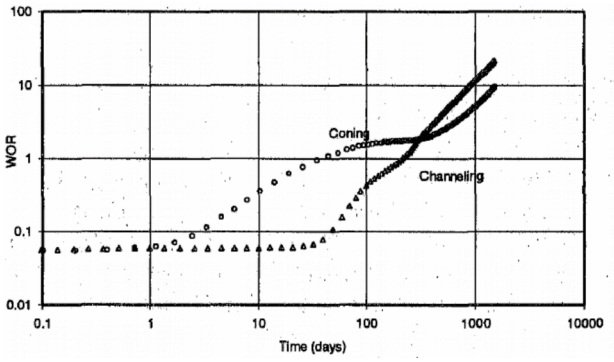


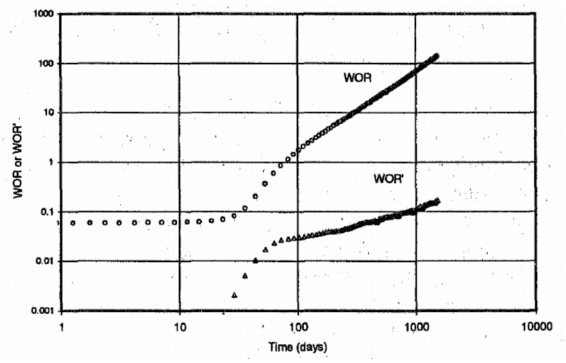


**Fig 2.11:** Water coning and channeling WOR comparison (Chan, 1995).

**Fig 2.12:** Multilayer channeling WOR and WOR' derivative (Chan, 1995).

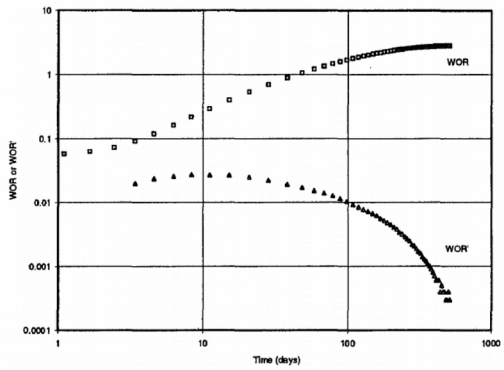


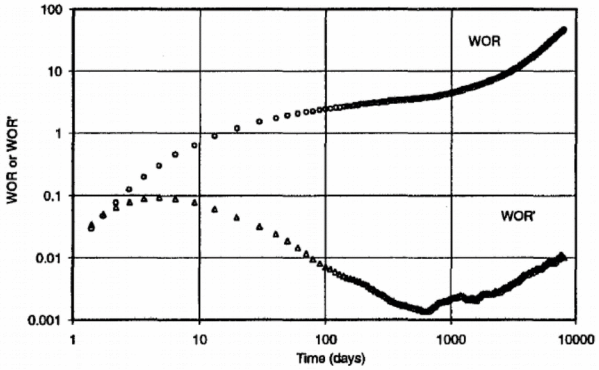


**Fig 2.13:** Bottomwater coning WOR and WOR' derivaties (Chan, 1995).

**Fig 2.14:** Bottomwater coning with late time channelling (Chan, 1995).

The use of diagnostic plots is widely accepted for wellbore and reservoir performance investigation. However, Seright, (1998) challenged the authenticity of the WOR plots as a tool for identification of excess water production mechanisms. Seright conducted research to determine the general applicability of the methodology proposed by Chan (1995). The outcome of Seright's research was partial disapproval of the use of Chan's methodology for the identification of excess water production mechanism. Seright (1998) stated that the WOR and WOR derivative diagnostic plots are not generic and could easily be misinterpreted and should not be used alone to identify excess water production mechanism. Rabiei (2011) validated

Seright's claim and suggested the plot of WOR and WOR derivative against recovery factor (RF) to be used for the identification of excess water production mechanism.

This research aims to apply artificial neural network (ANN) in extracting information from production data that aids prediction of excess water production mechanism, and forecast water cut over the productive reservoir life. ANN can work with noisy data and solve problems even if information related to detailed physics of the system of interest is not known or the system is too complex to be solved analytically (Nakutnyy *et al.,* 2008). Artificial intelligence can give the petroleum industry new tools for better understanding and controlling recovery processes and therefore achieving efficient and profitable oil recovery.

## 2.3 Overview of Artificial Neural Network

An artificial neural network is an information processing system that has certain performance characteristics in common with biological neural networks. A neural network is characterized by (1) its pattern of connections between the neurons (known as its architecture), (2) its method of determining the weight on the connection (known as training or learning algorithm), and (3) its activation function (Fausett, 1994).

The artificial neural network consists of an enormous number of interconnected simple processing elements called neurons, unit, cells, or nodes. The connection between neurons are weighted, and the weights represent information used by the network to solve problems. Neural networks have been applied in several areas including storing and recalling of data and pattern, performing general mapping from input patterns to output patterns, grouping of similar pattern, or finding solutions to the constrained optimisation problem (Fausett, 1994).

The characteristic mode of operation and function of the brain inspired the development of the neural network. The brain operates in a very complex manner consisting of approximately $10^{11}$ neurons of highly connected elements, approximately $10^4$ connections per element (Demuth *et al.,* 2014). These neurons have three principal components: the dendrites, the cell body (also known as soma) and the axon. Figure 2.15 shows a schematic representation of a biological neuron. The dendrites are a receptive network of nerve fibres that carry electrical signals into the cell body, the summation of these incoming signal threshold are done in the cell body, and the axon, which is a single long fibre, carries the signal from the cell body out to other neurons. A synapse is a point at which the axon of one neuron contacts the dendrite of another neuron.

The complexity in the manner in which the brain operates is enormously superior to that of an artificial neural network. However, there exist some similarities between the artificial and biological neural network. To start with, the building pieces of both networks are basic computational gadgets that are exceptionally interconnected, although artificial neural network is considerably less complex than biological neural network. Secondly, the connections between neurons decide the capacity and function of the network. Artificial neural networks are developed to mimic the biological neural system based on the following assumptions (Fausett, 1994).

1. Information is processed in many basic components called neurons.
2. Connection links enable transfer of signals between neurons.
3. Weights are associated with connection links; the weights multiply the signals transmitted.
4. To determine the output signal, each neuron applies an activation function to the net input signal.

Mathematically, the input signal can be expressed as the sum of the weighted inputs and bias.

$$network_k = \sum_{i=1}^{n} \left( w_{ki} * x_i \right) + b_k \quad (2.1)$$

Where $w$ is the weight, $x$ is the input data, and $b$ is the bias. The bias is like a weight, with the exception of its constant value of one, that shifts the transfer or activation function to the right or left.

**Table 2.2:** Terminological relationship between artificial and biological neurons (BuKhamseen, 2014).

| **Biological Neurons** | **Artificial Neurons** |
|---|---|
| Neurons | Node/Unit/Cell/Neurons |
| Synapse | Connection/Edge/Link |
| Synaptic Efficiency | Connection strength/Weight |
| Firing Frequency | Node output |

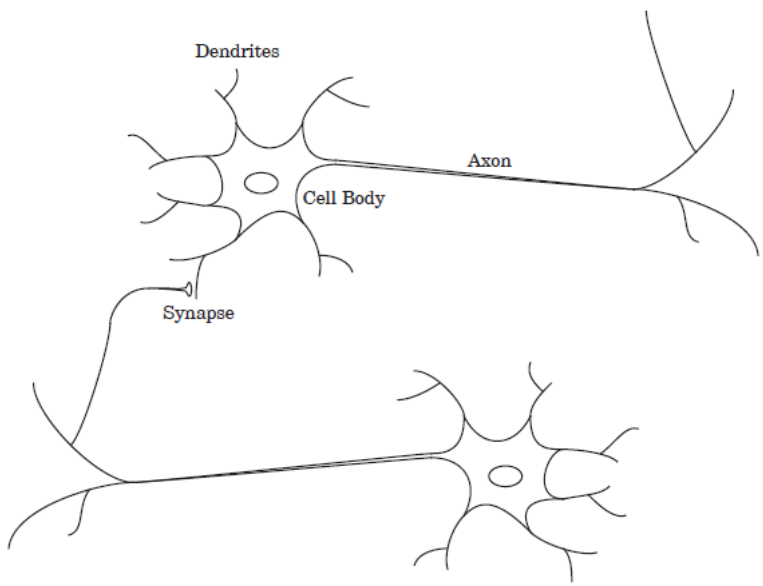


**Fig 2.15:** Schematic representation of a biological neuron (Demuth *et al.,* 2014).

Notwithstanding, if one prefers not to have a bias in a specific neuron, it can be discarded. It is worthy of note that both $w$ and $b$ are adjustable parameters of the neuron. The processed signal is

sent to the output node through a transfer function. The terminological relationship between artificial and biological neural network is shown in Table 2.2**.**

### 2.3.1 Brief History of Artificial Neural Network

The advancement in neural network development has occurred with several hitches rather than a smooth evolution. Some of the significant background work for the field of neural network occurred in the late 19$^{th}$ and early 20$^{th}$ century. Around that period, emphasis was mainly on the general theories of learning, vision, conditioning, etc., and did not include specific mathematical models of neuron operation (Demuth *et al.,* 2014).

A new phase of research in neural network began in the 1940s with the work of McCulloch, W. S. & Pitts, W. (1943). They suggested that the relation among neural events can be treated using propositional logic and further discussed the various application of calculus involved. Their work is often acknowledged as the origin of the neural network field (Demuth *et al.,* 2014).

Rosenblatt in (1958) was the first to practically apply the concept of artificial neural network by inventing the perceptron network and associated learning rule. He tried to understand the capability of higher organisms to recognise, generalise, recall, and think by trying to provide logical explanations to two fundamental questions: what form is information stored or remembered, and how does information in memory influence recognition and behaviour? Rosenblatt built a perceptron network that was able to perform the simple task of pattern recognition, and his success generated much interest in the research area. Unfortunately, the basic perceptron network developed by Rosenblatt could only solve a limited class of problems. Neural network-related research was suspended for about a decade because there were no powerful digital computers on which to experiment. In the 1970's, there was limited progress in the development of new neural network ideas within the scientific community. Fortunately,

things turned around for the better in the 1980's. Research in the neural network was reinvigorated because of the computational revolution that occurred during this period, and two new main concepts were developed: the use of statistical machines to explain the operation of a particular class of recurrent network, and the development of backpropagation algorithm for training multilayer perceptron networks. Recent advances in the neural network have had to do with new concepts, such as innovative architecture and training rules.

### 2.3.2 Artificial Neural Network Architecture

Complex problems may require layering of several neurons operating in parallel to obtain reasonable solutions. The layered arrangement of these connected neurons defines the architecture of the artificial neural network (Alghazal, 2015). There are three classes of a neural network: single layer feedforward network, multilayer feedforward network, and recurrent network.

#### 2.3.2.1 Single Layer Feedforward Network

A single layer network includes the weight matrix, the summers, the bias vector $b$, the transfer function boxes, and the output vector. The weight matrix $w$ connects every element in the input vector $p$ to each neuron. Each neuron has a bias $b_i$, a summer, a transfer function $f$, and an output $a_i$. The output from each neuron when put together forms the output vector $a$. A single layer network has only one hidden layer as suggested by its name. It is referred to as feedforward because the hidden layer is connected to the input vector and for the case of multi-layered network, the subsequent layer is connected to the previous layer. A schematic representation of a single-layered network is shown in Figure 2.16.

#### 2.3.2.2 Multilayer Feedforward Network

Multilayer neural networks usually have one or more layers between the input and output layer known as hidden layers (Fausett, 1994). Each layer has its own weight matrix, bias vector, a net input vector and an output vector. Problems that are complex to handle by a single layer network can be handled by a multilayer network. However, training of the network may be difficult. Figure 2.16 shows the schematic representation of a multilayer network architecture.

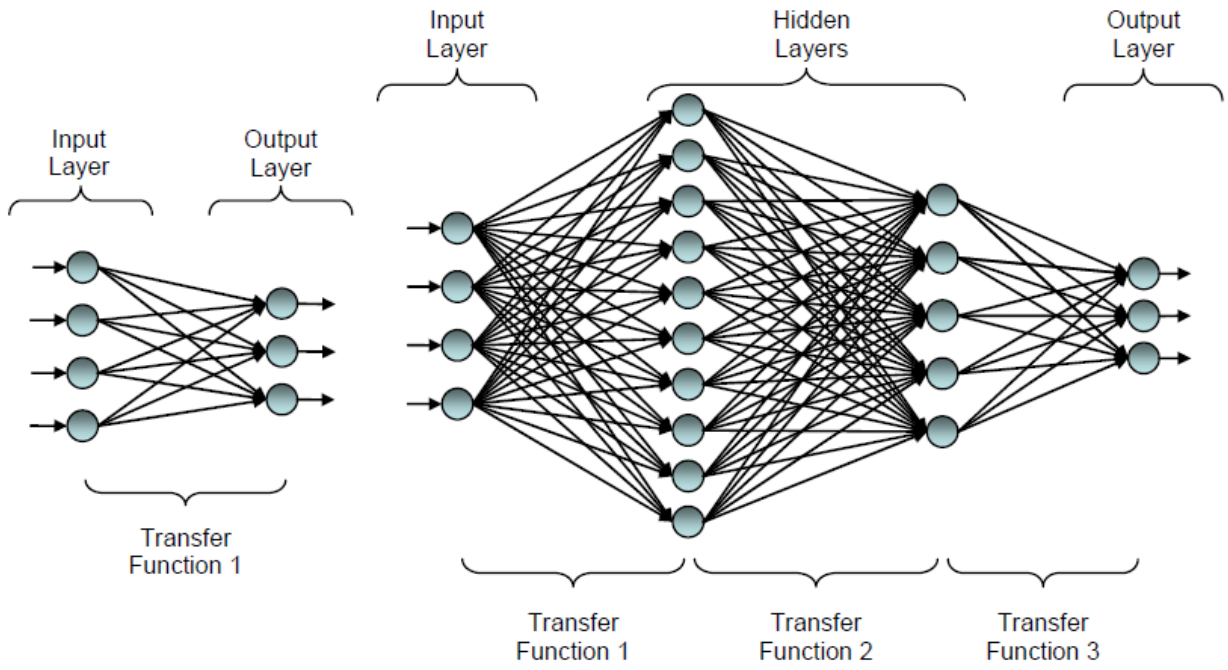


**Fig 2.16:** Single and Multilayer neural network architecture (Parada, 2008).

#### 2.3.2.3 Recurrent Networks

Recurrent networks have at least one feedback loop; this makes them different from the feedforward network in the sense that some of the outputs are connected to the input. The output of the recurrent network is the input delayed by one step, and the future outputs of the network

are computed from future outputs. Recurrent networks are potentially more powerful than feedforward networks (Demuth *et al.,* 2014).

### 2.3.4 Transfer function

A transfer function basically scales the response of a neuron to an external stimulus and generates the neuron activation (Maren *et al.,* 1990). Transfer function could be broadly classified as linear or nonlinear. The transfer fraction employed for solving problems depends on the complexity of the problem. Complex problems require the use of a multilayer neural network architecture, and a multilayer network requires the use of a nonlinear activation function. Most times, for a given layer, the same activation function is applied to all neurons, but for special cases different activation functions may be applied to a single layer. The most frequently used transfer functions are in multilayer networks are the linear (or purelin) and the sigmoid (logsig) transfer functions (Alghazal, 2015).

The purelin transfer function is a linear function that is mostly associated with the output layer since the network can produce within the desired limit without having to denormalize them (Minakowski, 2008). Sigmoid functions (S-shaped curves) are powerful continuous nonlinear transfer functions. The most commonly used sigmoid function are the logistic function and the hyperbolic tangent function. They are most helpful when used in a neural network trained by backpropagation, this is because there exists a simple relationship between the value of the function and its derivative at a point which reduces the burden of computation during training. The logistic and hyperbolic tangent function respectively take the input signal, which may lie between plus or minus infinity, activates the neuron, and scales the output signal within the range of (0 and 1), and (-1 and 1). Table 2.3 shows a list of activation functions.

**Table 2.3:** Transfer functions (Demuth *et al.,* 2014)

| Name | Input/Output Relation | Icon | MATLAB Function |
|---|---|---|---|
| Hard Limit | $a = 0 \quad n < 0$<br>$a = 1 \quad n \geq 0$ | | hardlim |
| Symmetrical Hard Limit | $a = -1 \quad n < 0$<br>$a = +1 \quad n \geq 0$ | | hardlims |
| Linear | $a = n$ | | purelin |
| Saturating Linear | $a = 0 \quad n < 0$<br>$a = n \quad 0 \leq n \leq 1$<br>$a = 1 \quad n > 1$ | | satlin |
| Symmetric Saturating Linear | $a = -1 \quad n < -1$<br>$a = n \quad -1 \leq n \leq 1$<br>$a = 1 \quad n > 1$ | | satlins |
| Log-Sigmoid | $a = \frac{1}{1 + e^{-n}}$ | | logsig |
| Hyperbolic Tangent Sigmoid | $a = \frac{e^{n} - e^{-n}}{e^{n} + e^{-n}}$ | | tansig |
| Positive Linear | $a = 0 \quad n < 0$<br>$a = n \quad 0 \leq n$ | | poslin |
| Competitive | $a = 1$ neuron with max $n$<br>$a = 0$ all other neurons | C | compet |

### 2.3.5 Learning Methods and Training Algorithm

Learning is the end product of a successful training procedure that is achieved by modifying the connection weights between nodes and biases of a neural network. Learning methods can be classified into supervised and unsupervised learning, there's, however, a third category where the weights are fixed without an iterative training process (Fausett, 1994). Supervised learning requires that an input vector or pattern be provided with its associated target or output vector or pattern. The weights are initialised to a small random number or zero; the weights are then iteratively manipulated until the calculated output vector is like the initial output vector within some acceptable range of error. The unsupervised learning does not require an output vector; the weights are modified such that the most similar input vector are assigned to the same target output.

Mathematical functions that are responsible for adjusting the weights and biases of the network are referred to as Training Algorithm. A number of training algorithms exist, including the Levenberg-Marquart (LM) algorithm, the gradient descent methods, the resilient backpropagation algorithm, the conjugate gradient methods, Newton's method and the Quasi Newton's method. Most oil and gas applications employ the feedforward network with backpropagation supervised learning algorithm. The backpropagation algorithm is a gradient descent method that minimises the total error between the output of the network and the desired targets by adjusting weights and biases using a generalised rule of the least mean square error (LMS) (Faussett, 1994).

Several training algorithms for multilayer feedforward backpropagation networks are present in the MATLAB neural network toolbox. Trainlm (Levenberg-Marquardt) is the default training algorithm used in this research. However, this algorithm is not suitable for training large complex

data set. ***Trainscg*** (Scaled Conjugate Gradient) and ***Trainrp*** (Resilient Backpropagation) are more frequently used for large data set. They both have relatively small memory requirements and are much efficient compared to other algorithms (Beale *et al*., 2017).

### 2.3.6 Convergence, Training Efficiency, and Overfitting

**Convergence** is said to take place when the total error of the current iteration is lower than the previous iteration. When the error between the desired and calculated outputs is minimised to a certain threshold, final convergence is said to have occurred. Convergence problem arises when the network calculates a lower total error as compared to that of the previous iteration. However, a global minimum is not reached due to the presence of at least local minima on the error surface. Training efficiency can be improved and made less sensitive to local minima on the error surface by combining techniques such as functional links, batching, adaptive learning and momentum (BuKhamseen, 2014, Beale *et al.,* 2017).

The basis for the momentum technique is the possible smoothing of the oscillation in the error trajectory. Consider the following first order filter (Equation **2.2**) to illustrate the momentum smoothing effect.

$$y(k)=\gamma y(k-1)+(1-\gamma)w(k) \quad 2.2$$

Where $w(k)$ is the input to the filter, $y(k)$ is the output of the filter and $\gamma$ is the momentum coefficient that must satisfy

$$0 \leq \gamma < 1 \quad 2.3$$

Figure 2.17 shows the effect of this filter. For the illustration, the input filter is a *sine* wave (Equation 2.4).

$$w(k)=1+\sin\left(\frac{2\pi k}{16}\right)2.4$$

A decreased oscillation can be observed when comparing the filter input and output, and as $\gamma$ increases, the oscillation in the filter output is reduced. The average filter output and input are the same, although the filter output is slow to respond as $\gamma$ is increased. In summary, the filter tends to reduce the number of oscillation while tracking the average value.

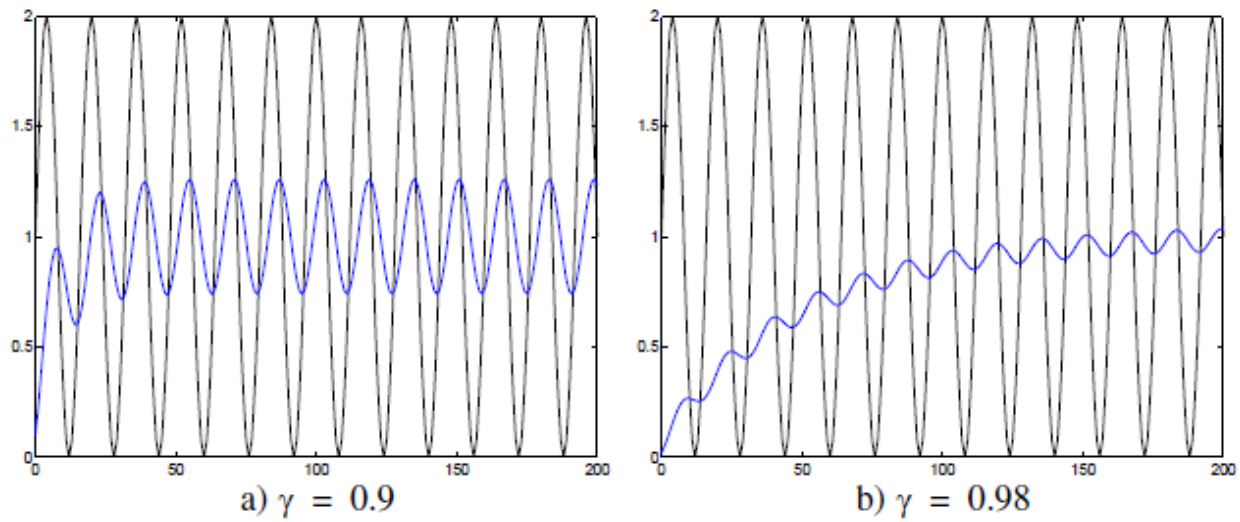


**Fig 2.17:** Smoothing effect of momentum (Demuth *et al.,* 2014)

Training efficiency can also be improved upon by altering the learning rate. Large learning rates lead to faster training, although some degree of fluctuation may be introduced. Small learning rates provide a more stabilised but delayed learning process, and this may direct convergence to a local minimum (Parada, 2008). The number of hidden layers chosen, and the number of neurons in each hidden layer affects the convergence speed. Choosing a number of neurons less than the required number leads to underfitting, while too many neurons may lead to overfitting (BuKhamseen, 2014).

**Overfitting** is one of the major problems during neural network training. Overfitting occurs when the error on the training set is driven to a small value but results in a large error when the network is presented with new data. This is as a result of the memorisation of the trained examples rather than learning to generalise to new situations. Regularisation and early stopping are techniques used for preventing memorisation and improving generalisation (Beale *et al.,* 2017).

In early stopping, the available data is divided into three subsets, namely: training, validation, and testing data set. The training data set is used for computing the gradient and updating the weights and biases. The validation data set is used to detect data overfitting. During the training process, the error on validation is monitored, and this error normally decreases during the initial phase of training, and so does the training error. However, overfitting of data by the network results in an increase in a validation error. Training terminates when the validation error increases for a specified number of iterations, and the weights and biases at the minimum of the validation error are returned. The test data set is not used during the training process, it measures the ability of the network to generalise. The lower the error of this subset, the better the network's generalisation capability.

Regularisation involves modification of the performance function which is usually chosen to be the sum of squares of the network error on the training set. The mean sum of square is the typical performance function used for training feedforward neural networks.

$$F = mse = \frac{1}{N}\sum_{i=1}^{N}(e_i)^2 = \frac{1}{N}\sum_{i=1}^{N}(t_i - \alpha_i)^2 2.5$$

Where $N$ is the number of inputs, $e$ is the error function, $t$ is the target value, and $\alpha$ is the output value. There is a possibility to improve generalisation by modifying the performance function.

This is done by adding a term consisting of the mean sum of squares of the network weights and biases.

$$msereg = \gamma * msw + (1-\gamma) * mse \quad 2.6$$

Where $\gamma$ is the performance ratio which has a value between 0 and 1, and

$$msw = \frac{1}{n}\sum_{j=1}^{n} w_j^2 \quad 2.7$$

Application of the performance function results to a reduction in the magnitude of the network weights and biases, and this forces the network to respond in a smoother manner that is less likely to overfit (Beale *et al.,* 2017).

### 2.3.7 Application of Artificial Neural Network in the Oil and Gas Industry.

BuKhamseen (2014) developed an artificial expert system, which provides the reservoir engineer with a good set of starting points to pick the history matching parameters for a newly created reservoir simulation model. The developed expert system showed great flexibility when handling temporal changes that occurred during the life of the reservoir.

Parada (2008) developed artificial neural networks that are used to build two neuro-simulation tools for screening and designing miscible injection, waterflooding and steam injection processes. The neuro-simulation tools are intended to narrow the ranges of possible scenarios to be modelled using conventional simulation, reducing the potentially extensive time and energy spent in modelling studies and analysis.

Hegeman *et al.,* (2009) applied artificial neural network to downhole fluid analysis. They developed an artificial neural network model that uses the downhole fluid analysis tool

measurements of fluid composition as inputs to predict the gas/oil ratio. The model also provided an uncertainty estimation of its outputs as a quality assurance indicator.

Nakutnyy *et al.,* (2008) applied a neural network for analysing data from a Canadian oil field that had been under waterflooding for several years. Production data for the last 20 years were used to develop the neural network, and the neural network developed could predict future oil recovery from waterflooding.

Panda *et al.,* (1996) applied artificial neural network to model gas-oil contact movement in Prudhoe Bay reservoir. They used oil, gas, and water production, perforation history, permeability, sand and shale distribution, and surveillance data at surrounding wells as artificial neural network input to predict the fluid distribution at a target well. They observed that the neural network is capable of predicting fluid distribution at a target well more accurately and consistently than conventional methods.

Saeedi *et al.,* (2007) used field data to develop a neural network model to identify candidate wells and predict well performance for water shutoff treatments using polymer gels. The developed neural network could accurately predict the post-treatment cumulative oil production of the well one month after treatment with an average error of 16%, and the post-treatment cumulative oil production three months after treatment with an average error of 10%.

Njoku *et al.,* (2013) applied the neural network approach to facies modelling as part of the static modelling workflow for several turbidite reservoirs in an offshore Nigerian oil field. The key input data applied to delineate and model the facies were cores, well logs, and seismic. They concluded that a neural network approach is a reliable tool for modelling deep-water facies with better connectivity, higher repeatability and requires short turnaround time.

Al-Bulushi *et al.,* (2007) developed and tested a methodology based on artificial neural network models to predict water saturation using wire-line logs and core Dean-Stark data. They presented a detailed workflow for developing ANN models for sandstone reservoirs, where conventional wire-line logs are taken as input parameters.

Sunday (2016) developed and used ANN models as a reservoir management tool to proffer solution to excess water problem. The developed models were able to predict well water cut, with accuracy as high as 92.2%. The developed neural network model results were used alongside reservoir simulation to suggest possible ways of mitigating excess water production.

The oil and gas industry is hungry for possible solutions to the problem of excess water production. A review of the literature indicates that most of the existing approaches to solving this problem have seen minimal success in field application. This points to the fact that excess water production remains a conundrum that awaits a new and efficient approach to mitigate. During this research, we leveraged on the existing foundation laid by Sunday (2016) by employing a data-driven approach to solve the problem of excess water production in the oil and gas industry. The proposed data-driven approach is discussed in the next chapter.

# CHAPTER THREE

## 3.0 METHODOLOGY

### 3.1 Overview

This research focuses on building a neural network model that can be used to predict water cut of different wells for a given reservoir. Figure 3.1 shows a schematic representation of the research methodology. For data gathering, a reservoir (base) model was built using Eclipse simulation software (Schlumberger, 2017). Several modifications were made to the base reservoir model to simulate different reservoir behaviour compared to the base model. After collection of the required data, a neural network model was then built to predict water cut for individual wells placed in the reservoir models.

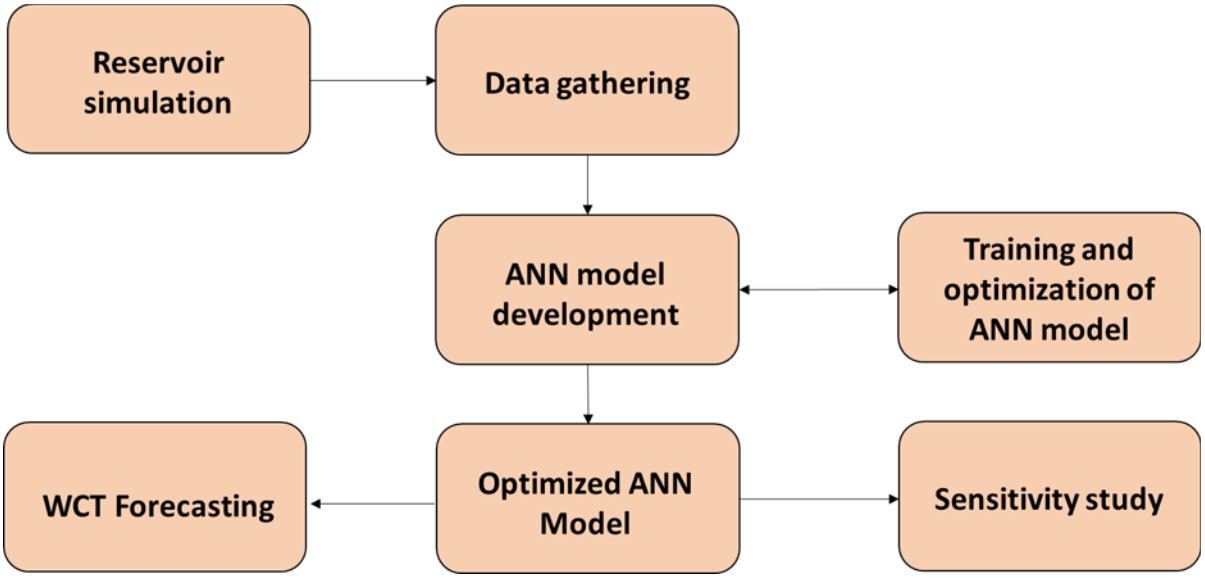


**Fig 3.1:** Research Methodology

### 3.2 Base Reservoir Model

The reservoir simulation model used in this research is patterned after the Ninth SPE comparative solution project (Killough, 1995). The base model was modified to collect production data used in building the neural network model. Some of the changes made to the model include reservoir permeability homogenization, introduction of an active aquifer to maintain reservoir pressure and to bring about water encroachment into the producers in addition to the water introduced into the reservoir by the injectors. A total of 10 wells, including six producers and four injectors, were drilled in the reservoir model (Figure 3.2). Table 3.1 shows the properties of the modified reservoir model.

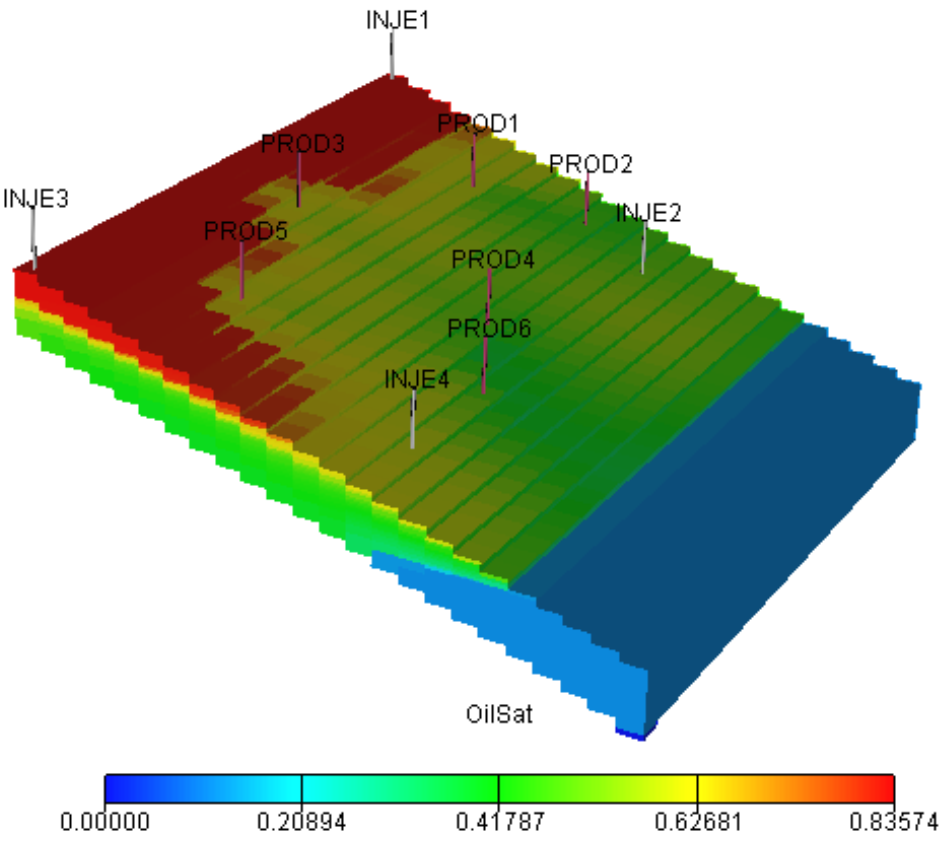


**Fig 3.2:** Reservoir model

**Table 3.1:** Modified reservoir model properties

| | |
|---|---|
| Model Dimensions | 24 * 25 * 16 |
| Grid Size (DX * DY), ft. | 300 * 300 |
| DZ, ft. | 8 – 100 |
| Kx = Ky , md | 108 |
| Kz=0.1Kx , md | 10.8 |
| Aquifer initial pressure, psia | 6000 |
| Datum depth, ft. | 9035 |
| Datum pressure, psia | 5000 |
| Simulation time, years | ≈ 26 |

### 3.3 Neural Network Model

A nonlinear autoregressive neural network (NARXNET) model was used in this study. The nonlinear autoregressive neural network with external input model, when supplied with past values of a time series, can learn to predict that time series. The model relates current values of the time series to both the past values of the same time series and an externally determined series to obtain values of the series of interest.

Sunday (2016) researched the application of artificial neural network for forecasting well water cut using a nonlinear autoregressive neural network with external input (NARXNET) model. His work showed that the ANN model could predict well water cut with a high level of accuracy (up to 98.11%) if the right input parameters are supplied in the process of building and training the neural network model. The stronghold of this research is to investigate the sensitivity of an ANN model to various changes in reservoir property.

Two NARXNET models (NET1 and NET2) were developed in this research. NET1 was built to forecast the well water cut of a reservoir, after supplying the neural network model with past production data. NET2, on the other hand, was built to predict the well water cut of a reservoir

where there are changes in reservoir properties or operational parameters. For example, changes in reservoir permeability, aquifer pressure, and the rates of oil and gas production.

The models had a total of 25 input parameters, input and feedback delay was 2, the number of hidden layers was 10, and one output layer. The transfer function in each of the hidden layers was the log sigmoid (logsig) transfer function, while the transfer function in the output layer was a linear transfer function, the purelin transfer function.

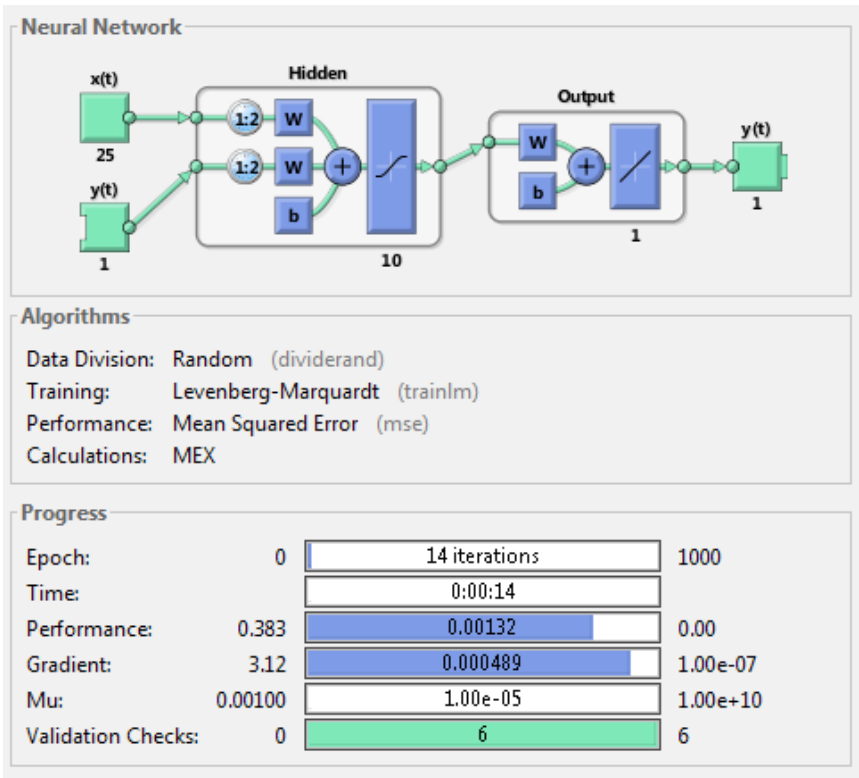


**Fig 3.3:** Artificial neural network model parameters

The neural network model training algorithm is the Levenberg-Marquardt (lm) training algorithm with a learning rate of 0.05, the number of epochs is 300, and the training goal is 0.00001, and the performance function is the mean square error (mse). The input data were randomly divided into training, testing and validation data, in the ratio of 70:15:15. Figure 3.3 shows the training

GUI with the neural network model parameters, while Figure 3.4 and Figure 3.5 show the regression coefficients after training of NET1 and NET2 models, respectively.

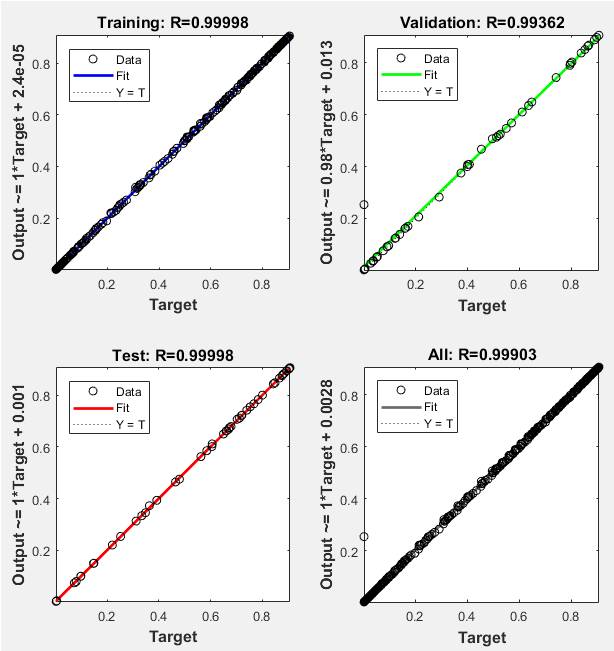


**Fig 3.4:** Training, validation, testing and overall regression coefficient of NET1

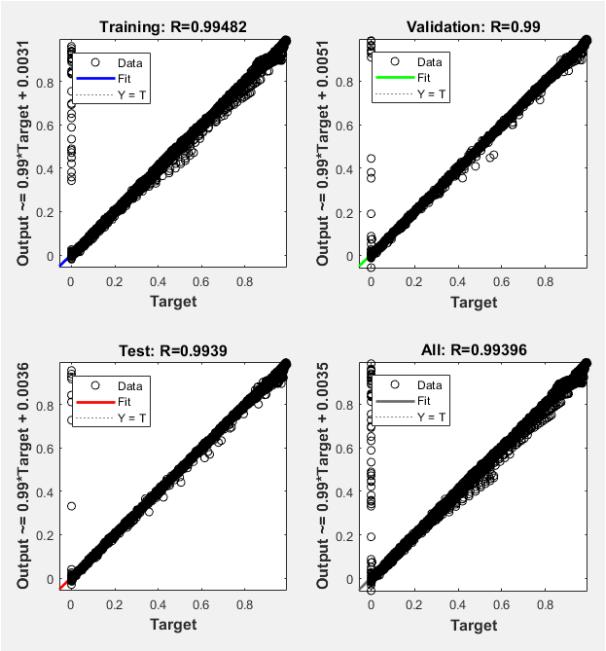


**Fig 3.5:** Training, validation, testing and overall regression coefficient of NET2

A total of 25 reservoir parameters served as input to the neural network model. See appendix (A) for a list of the input parameters to the neural network model, and the reservoir conditions at which these input parameters were obtained.

### 3.4 Well Water Cut Forecast

Net1 was built for forecasting water cut of a well. To develop this model, production data was obtained from one of the wells (P6) in the reservoir described in section 3.2 of this work. The effect of a water injection process was not of interest at this point, so the injectors were turned

off. The model described in section 3.2, with inactive injectors will from now on be referred to as the base model.

The base reservoir model was built, and oil production was simulated for a period of 26 yrs. The input data to NET1 was obtained from the simulation results and used to populate a spreadsheet. The first 22 years of simulation data were used to build and train NET1, while the last 4 years of simulation were forecasted by NET1. The forecasted results for the last 4 years of production by NET1 and the results from the simulation were then compared to determine the accuracy of prediction by NET1.

### 3.5 Sensitivity Study

NET2 was built to investigate the sensitivity of the neural network model to changes in reservoir property. This was achieved by building and training NET2 using production data obtained from all producers in the reservoir model, and then predicting the water cut profiles of those producers after introducing changes in the properties and operational parameters of that reservoir model. The altered parameters in the reservoir model include permeability contrast, horizontal permeability, perforation interval of producers, the distance between the injector and producer, and the initial aquifer pressure.

#### 3.5.1 Sensitivity of the NN model to change in permeability contrast ($k_v/k_h$)

The $k_v/k_h$ value of the base model is 0.1 as shown in Table 3.1. To carry out this sensitivity analysis, every reservoir parameter remained the same as that of the base model, except for the $k_v/k_h$ values. Three $k_v/k_h$ values of 0.01, 0.5 and 1 were used. The ANN training dataset were obtained from the simulation results of models with $k_v/k_h$ values of 0.01, 0.1, and 1. To validate

the ANN model, the well water cut of all producers in a reservoir model with $k_v/k_h$ value of 0.5 were predicted. The results obtained from simulation were then compared to the prediction by NET2 for the reservoir model with $k_v/k_h$ of 0.5.

Sensitivity studies with regards to change in permeability contrast were done to determine the ability of the neural network model to predict well water cut in a reservoir considering different degrees of restriction to fluid flow in the vertical direction. In the reservoir model, the producers are perforated in Layer 2 – 4, the injectors are perforated in Layer 11 – 15, and a bottom water drive exist. Itwas expected that the flow pattern and behaviour of water travelling upward from the aquifer and injectors toward the producers would differ for various $k_v/k_h$. It was expected that changes in $k_v/k_h$ values would impact the well water cut profiles observed at the producers.

### 3.5.2 Sensitivity of the NN model to change in horizontal permeability ($k_h$)

The base reservoir model is a homogeneous reservoir with a horizontal permeability of 108md. To investigate the effect a change in horizontal permeability will have on the outcome of the prediction by NET2, three other reservoir models having horizontal permeability values of 400md. 800md and 1200md were built and simulated.

Production data obtained from the simulation of reservoir models with $k_h$ values of 108md and 800md served as training data for NET2. NET2 was then used to predict the water cut profile of all the producers in the reservoir with kh values of 400md and 1200md. The well water cut prediction by NET2 was then compared to the results obtained from the simulation.

The sensitivity of the neural network model to changes in horizontal reservoir permeability is important because, during production, the pore throats could get clogged by foreign material or

the reservoir fluid, bringing about a reasonable reduction in horizontal permeability. Also, acidification to reduce near wellbore skin reduction and sand production can improve the horizontal permeability near the production wells. The sensitivity study was to check the accuracy of the ANN model prediction when the reservoir horizontal permeability has been changed from its original value after some period of well production and/or changes to well operations.

### 3.5.3 Sensitivity of the NN model to the perforation interval of the producers

The producers in the base reservoir model were perforated in Layer 2 – 4. There could be a need to perforate a different set of layers to reestablish communication with the formation, especially in cases where an impermeable layer separates different layers in the pay zone. The predictability of the neural network relative to changes in perforation interval of the producers was investigated. Two reservoir models were built for this purpose. All producers were perforated at different layers. Input information to the neural network for predicting water cut was obtained from the simulation results of both models. The training data set were obtained from reservoir models where the producers were perforated at Layer 2 – 4 and Layer 6 – 8 (see Figure 3.6).

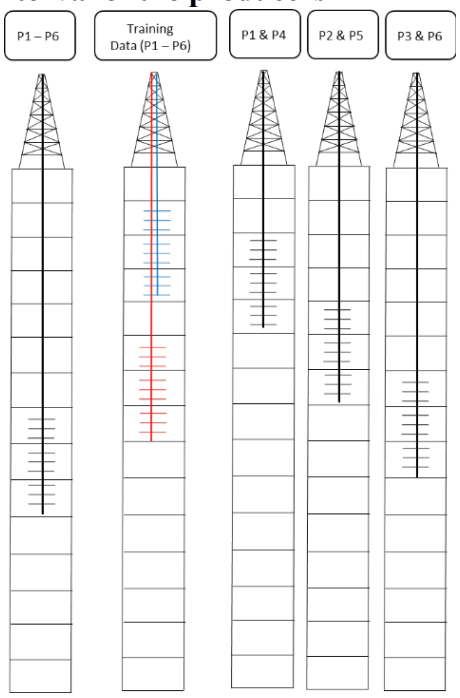


**Fig 3.6:** Schematic representation of the perforation intervals where training data were obtained and forecasting was done.

### 3.5.4 Sensitivity of the NN model to the distance between injector and producer

The distance between an injector and a producer determines the injection water breakthrough time, *ceteris paribus*. To study this impact, a sensitivity study of the separation distance between the injector and producer becomes important. The distance between the injector 3 and producer 5 in the base reservoir model is 1500 ft. Four other reservoir models were built, and the simulated separation distances between injector 3 and producer 5 are, 300 ft., 900 ft., 2100 ft., and 2700 ft.

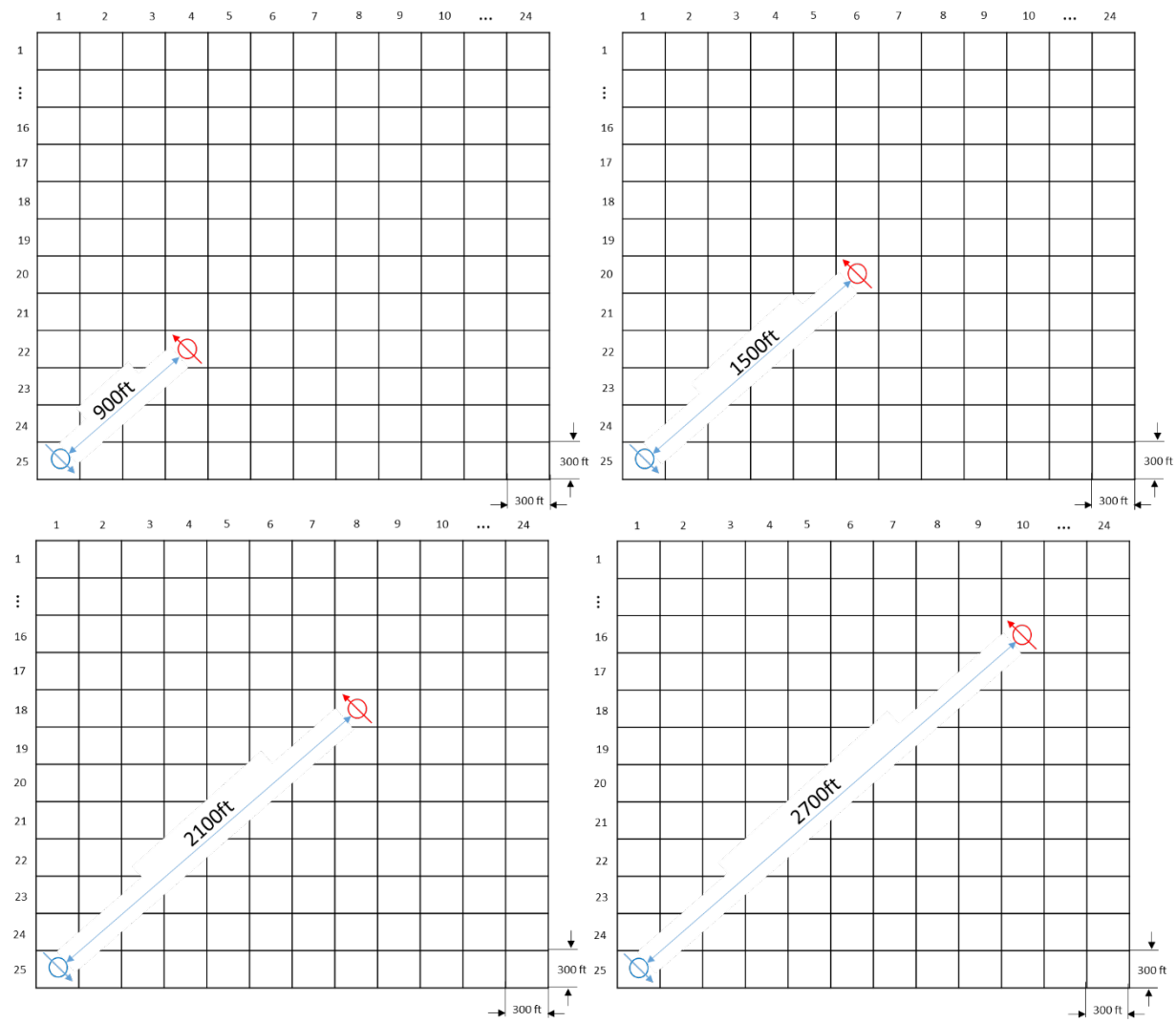


**Fig 3.7:** Schematic representation of the reservoir showing the various locations of the producers

The data for training the neural network model was obtained from the models where the distance of separation between injector 3 and producer 5 was 900 ft. and 1500 ft., respectively. After the training, water cut was predicted for producer 5 in the models considering separation distance between the injector 3 and producer 5 of 300 ft., 2100 ft., and 2700ft (see Figure 3.7).

### 3.5.5 Sensitivity of the ANN model to the initial aquifer pressure

The sensitivity of the neural network model to changes in the initial aquifer pressure of the reservoir was also investigated. The base model had initial aquifer pressure of 6000 psi, and three other reservoir models were built having initial aquifer pressure of 2000 psi, 4000 psi and 8000 psi, respectively. The training dataset was obtained from reservoir models with initial aquifer pressure of 2000 psi and 6000 psi, while the forecasting of well water cut was done by the neural network model for the models with initial aquifer pressure of 4000 psi and 8000 psi respectively. The forecast and predictions of NET1 and NET2 are discussed in the next chapter.

# CHAPTER FOUR

## 4.0 RESULTS AND DISCUSSIONS

### 4.1 Results of Well Water Cut Base Forecast

The results of the well water cut forecast for the base reservoir model are presented in this section. Recall as described in Chapter 3, for the base case study, a model was used to simulate water cut profiles for a reservoir that contained six producers and four injectors. The model was produced, and the simulation ran for 26 years, and the results of the first 22 years of production were used to train the NET1. NET1 forecasted the well water cut profile for the last four years. Figure 4.1 shows the training, testing, validation and overall regression coefficient after the successful training of NET1.

Fig 4.1 shows the results of the water cut at producer P6 from the reservoir model. The blue trend line represents the water cur profile obtained from the original/base case model. Cascaded on the water cut profile of P6 are the results obtained from the training, testing and validation of NET1 (black trend line). NET1 forecasted the results (red trend line in Figure 4.1) of the last four years. The results show that the water cut forecast of P6 by NET1 was a very good one, with a mean square error and regression coefficient of 1.5985e-05 and 0.9985 respectively.

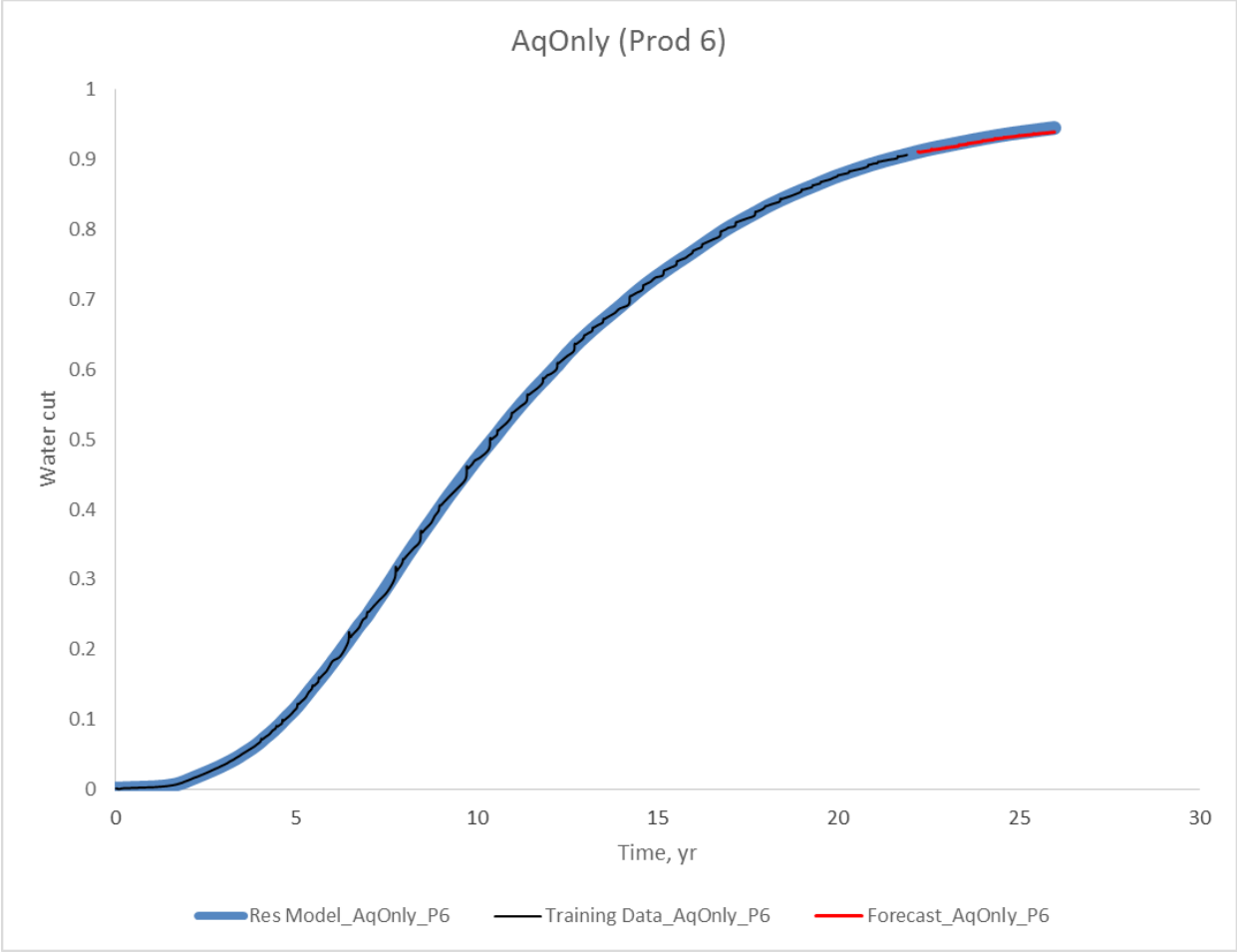


**Fig 4.1:** Water cut forecast of Prod 6 (P6) in the base reservoir model

## 4.2 Results of Sensitivity Study

Sensitivity studies were carried out using the neural network model (NET2) to study the impact of changes to several reservoir properties and operational parameters on the model forecast. The following changes were made during the sensitivity study: permeability contrast, horizontal permeability, perforation interval of producers, the distance between injector and producer, and the initial aquifer pressure.

### 4.2.1 Neural Network Model (NET2)

ANN model NET2 was used to carry out the sensitivity study. Input data used for training the neural network model was obtained from the base reservoir model. In the sensitivity cases, some of the base model properties were modified to evaluate the accuracy of the results forecasted by NET2 in the study. The detailed model input properties and data modifications are shown in the appendix (see Appendix A).

### 4.2.2 Results of Sensitivity of Artificial Neural Network Model to permeability contrast ($k_v/k_h$)

All models used for this sensitivity study were perforated in Layer 2-4, and all other reservoir parameters remain unchanged except for the $k_v$/kh. As the value of $k_v/k_h$ approaches unity from a much lower value of 0.01, it is expected that flow toward the wellbore in the vertical direction increases because there is less restriction to vertical flow.

Figure 4.2 shows the water cut profiles of Producer 1 (P1) obtained from the four models with different $k_v/k_h$ values. The $k_v/k_h$ values labelled A, B, C, and D in Fig 4.2 are 1, 0.5, 0.1 and 0.01, respectively. Data obtained from cases A, C and D, were used for training the neural network model, and the water cut profile for Producer 1 was predicted in case B only using the NET2 model. As expected, the earliest water breakthrough occurred just after five years of production in case A, and water breakthrough time for Producer 1 in case D which has the lowest $k_v/k_h$ value was after 18.5 years of production. From Figure 4.2, the blue trend line represents the water cut profile of Producer 1 obtained from the simulation of case B. Note, the data from this case B prediction run was not part of the neural network training data set. As shown in Figure 4.2, the simulation results (the blue line labelled case B) matched the results predicted by the neural network model (thin black line labelled case B). The neural network prediction was close to a

perfect match with a regression coefficient of 0.9999 and mean square error of 2.066e-05. Another evidence of the predictability power of the ANN models studied in this work.

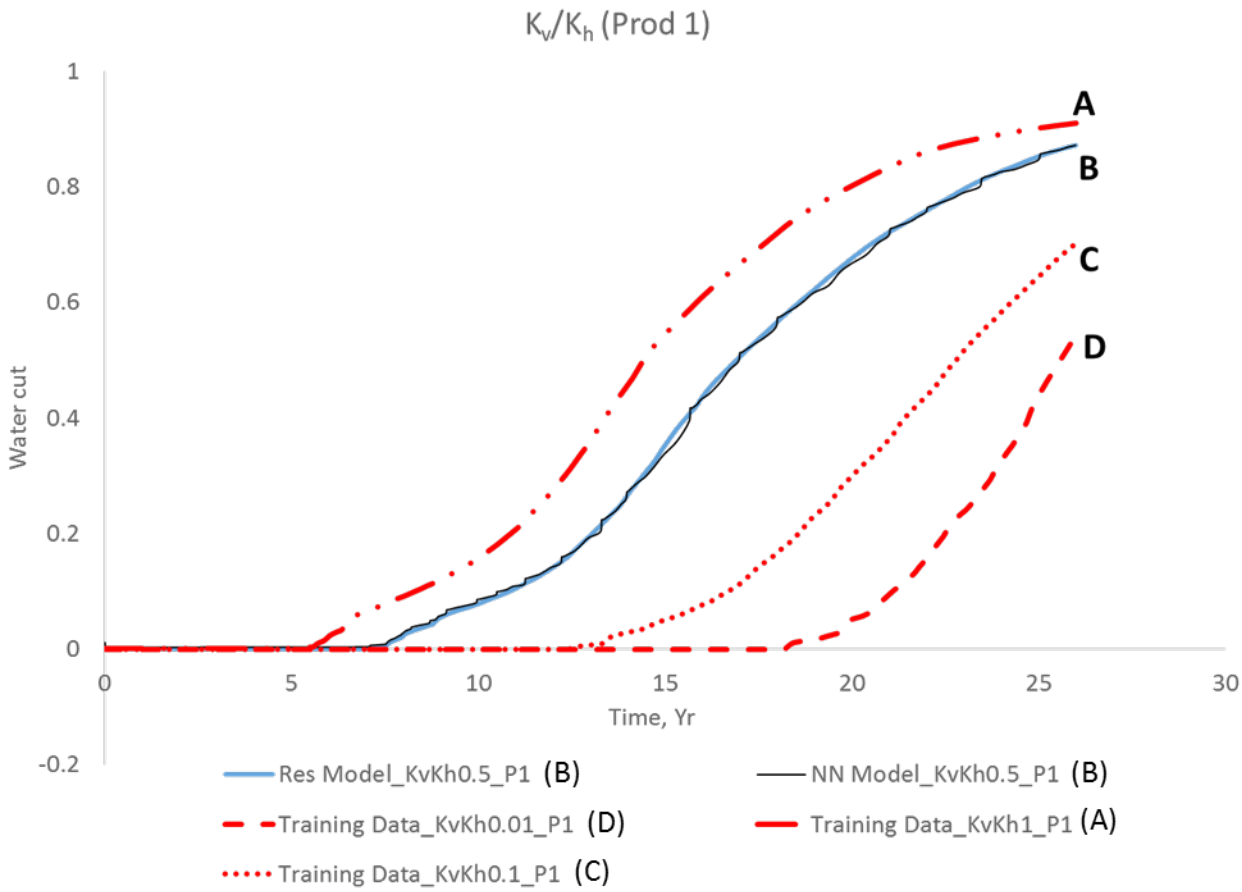


**Fig 4.2:** Water cut prediction of Prod 1 (P1) by NET2 with changes to reservoir permeability contrast, $K_v/K_h$

Figure 4.3 shows the simulation results for six producers in the reservoir model having $k_v/k_h$ values of 0.5. The figure also shows the results predicted by the ANN model. The data indicated that predicted results closely matched the simulation results as can be seen from the regression coefficients and mean square errors (Table 4.1).

**Table 4.1:** Regression Coefficients and Mean square errors from ANN Model for kv/kh=0.5 (Model Simulation vs. ANN Prediction for Kv/Kh=0.5)

| Producers | Regression Coefficients | Mean Square Errors |
|---|---|---|
| Prod 1 | 0.9999 | 2.066e-05 |
| Prod 2 | 0.9998 | 5.4587e-05 |
| Prod 3 | 0.9998 | 2.2840e-05 |
| Prod 4 | 0.9999 | 4.1660e-05 |
| Prod 5 | 0.9998 | 1.8682e-05 |
| Prod 6 | 0.9998 | 8.7441e-05 |

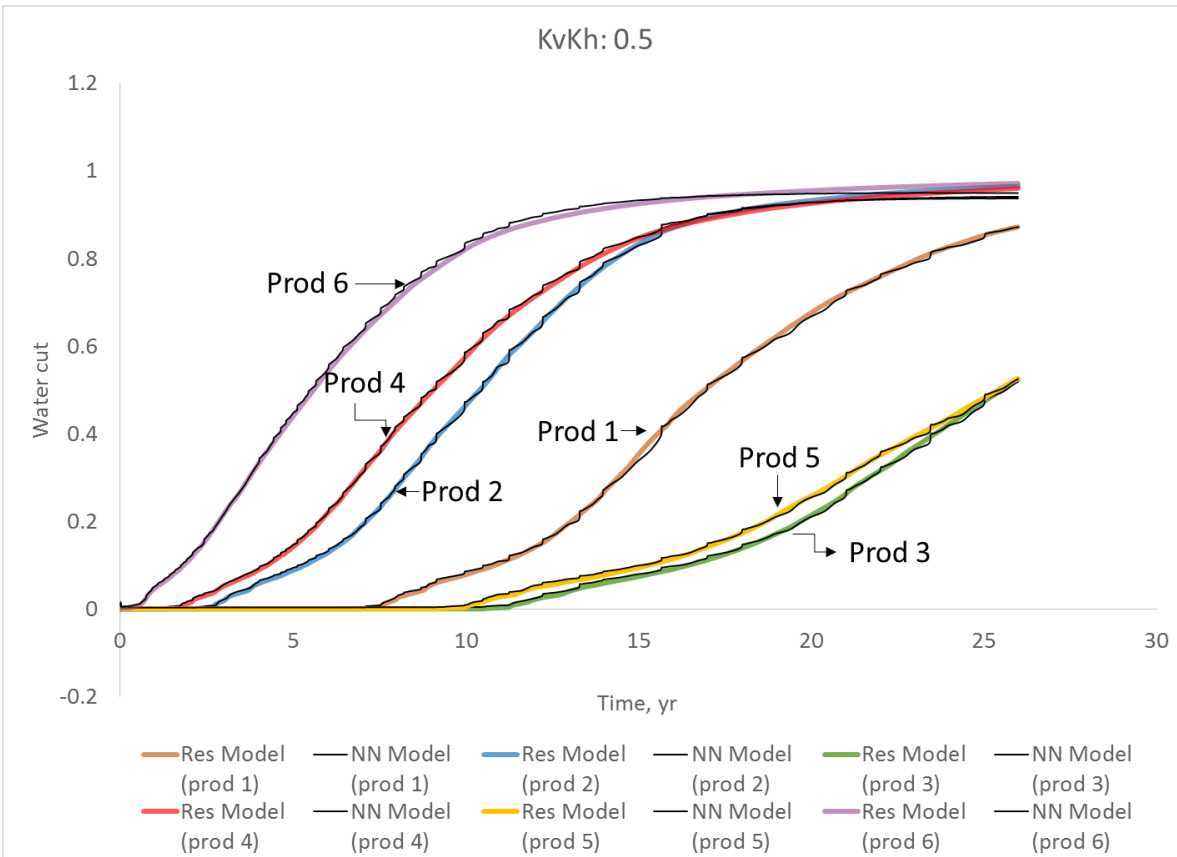


**Fig 4.3:** Water cut prediction by NET2 for all producers in a reservoir with $k_v/k_h$ of 0.5

### 4.2.3 Results of Sensitivity of Artificial Neural Network Model to horizontal permeability

The horizontal permeability controls the volume of fluid flow from the reservoir to the wellbore.

Several factors may alter the horizontal permeability as pointed out in section 3.4.2 of this thesis.

Thus, a sensitivity study of the results predicted from the neural network model considering changes in the reservoir horizontal permeability becomes important.

The neural network model training data set was obtained from the models with a horizontal permeability of 108md and 800md. The water cut profiles at the producers was predicted using the same reservoir model but with the horizontal permeability set equal to 400md and 1200md. Figure 4.4 shows the results of the well water cut for Producer 1 (P1) and Producer 2 (P2) comparing the training data versus the ANN model predictions. The red trend lines in Figure 4.7 are the training data for Producer 1 (P1) and Producer 2 (P2) obtained from the simulation case of a model with a horizontal permeability of 800md.

The results from the neural network model prediction for Producer 1 (P1) and Producer 2 (P2) in the reservoir with $k_h$ of 400md closely matched the simulation results ($k_h$ of 800md). The regression coefficients obtained are 0.9998 and 0.9996, and the mean square errors of 6.1040e-05 and 4.3133e-04, respectively, were obtained in this case. Notice that when the horizontal permeability of the reservoir used in the ANN model prediction was increased to 1200md, there was some reduction in the ANN's model accuracy. The prediction of water cut profiles for wells in the 120md permeability case was not a very close match as was the prediction for 400md reservoir. Figure 4.7 shows that the neural network model slightly overpredicted water cut during the first 21years of production of Producer 1 (P1), but the results showed improved accuracy in predicting the water cut during the remaining life of the well. Table 4.2 shows the regression coefficients and mean square errors for this 1200 md horizontal permeability case. Regression coefficients for prod 1 and prod 2 in the prediction of well water cut in the 1200md model are 0.9962 and 0.9994 respectively, while the respective mean square error is 7.0307e-04 and 6.1421e-04.

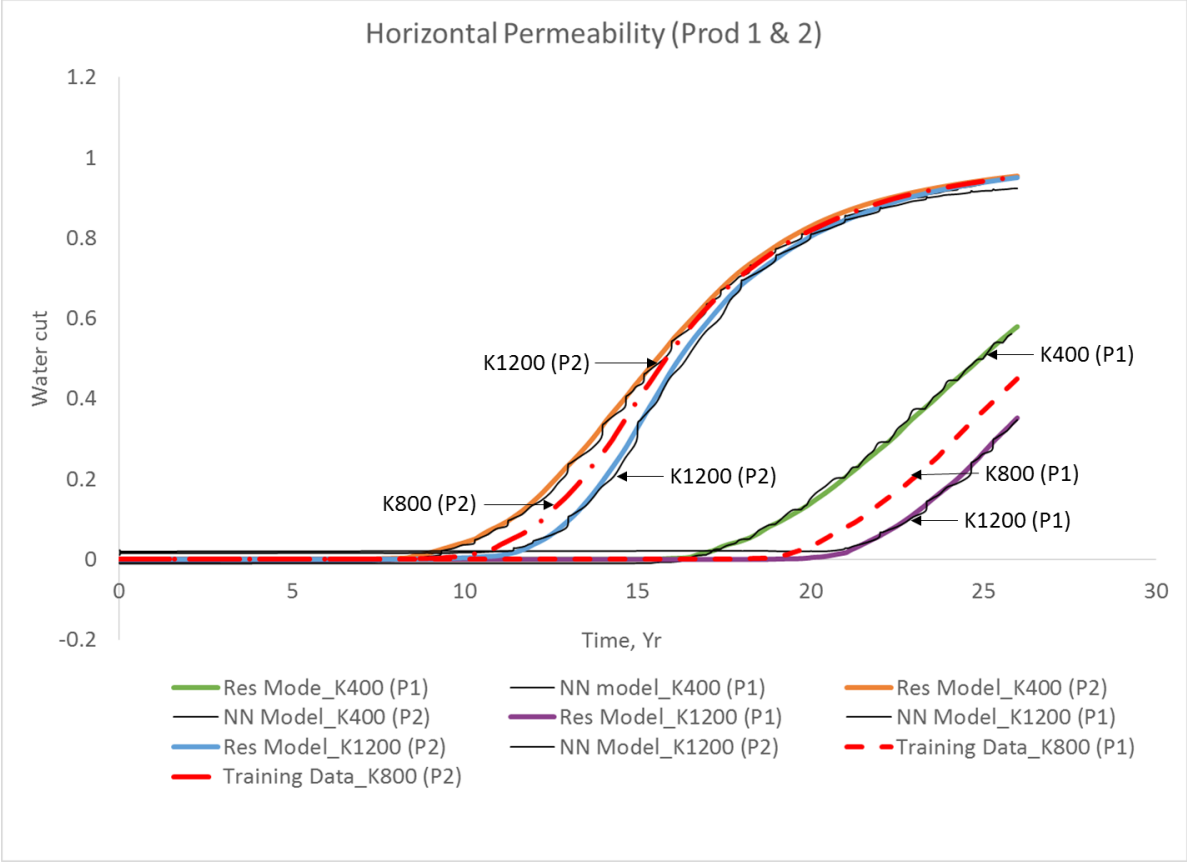


**Fig 4.4:** Water cut prediction of P1 and P2 by NET2 with changes to reservoir horizontal permeability

Figure 4.5 shows the simulation results for six producers in the model with a horizontal permeability of 400md. The simulation results and the prediction by the neural network model, are closely matched as can be seen from the regression coefficients and their mean square errors of Producer 3, Producer 4, Producer 5, and Producer 6 (See Table 4.2).

**Table 4.2:** Regression Coefficients and Mean square errors from ANN Model Prediction for kh=1200 md (Model Simulation vs ANN Prediction for Prediction Kh=1200 md)

| Producers | Regression Coefficients | Mean Square Errors |
|---|---|---|
| Prod 1 | 0.9962 | 7.0307e-04 |
| Prod 2 | 0.9994 | 6.1421e-04 |

| | | |
|---|---|---|
| Prod 3 | 0.9980 | 6.7897e-04 |
| Prod 4 | 0.9996 | 4.6135e-04 |
| Prod 5 | 0.9994 | 7.5470e-04 |
| Prod 6 | 0.9992 | 6.3735e-04 |

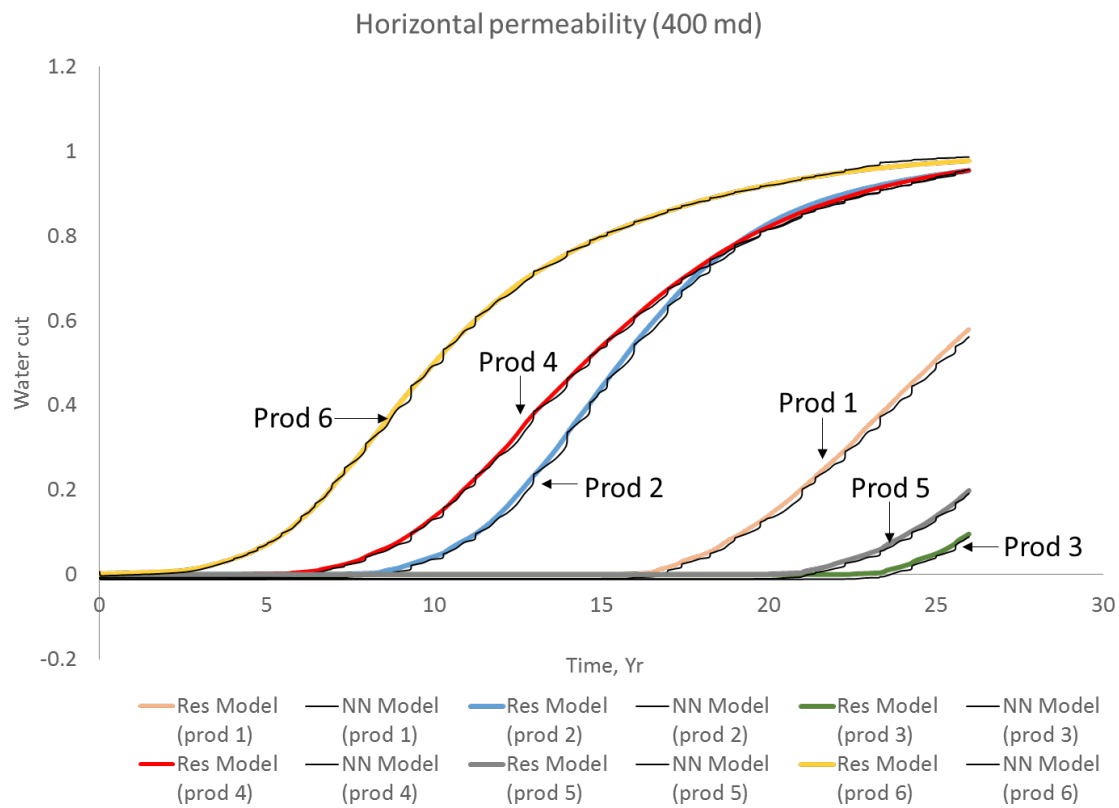


**Fig 4.5:** Water cut prediction by ANN model for all producers for case study with horizontal permeability of 400md

### 4.2.4 Results of Sensitivity of Artificial Neural Network Model to changes in perforation intervals

To study the impact of changes in perforation interval on the model predictive accuracy, the training data for the neural network was obtained from two reservoir models, one perforated in Layers 2 – 4 and the other perforated in Layers 6 – 8. Two other perforation intervals were used to predict the well water cut. Prediction was done for all wells in Reservoir (A), perforated in Layers 8 – 10, and in Reservoir (B) where the producers are perforated at different intervals. For

Reservoir (B), Prod 1 and Prod 4 were perforated in Layers 3 – 5, Prod 2 and Prod 5 were perforated in Layers 5 – 7, and Prod 3 and Prod 6 were perforated in Layers 7 – 9.

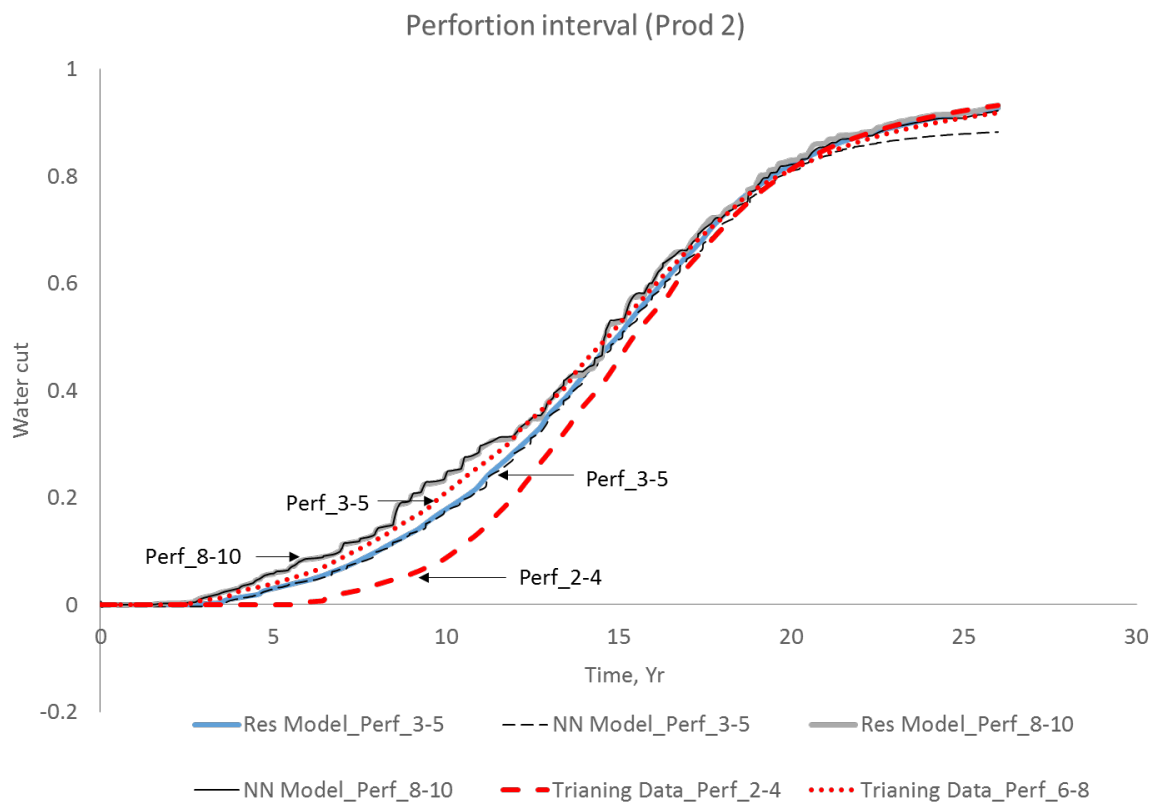


**Fig 4.6:** Water cut prediction of P2 by NET2 with changes to reservoir perforation interval

Figure 4.6 shows the results of well water cut profiles of prod 2 in all four reservoirs. Figure 4.7 shows the perforation intervals used in the training and forecasting with the NET2 model. In Figure 4.6, the red trend lines represent the training data set obtained from wells perforated in Layers 2 – 4, and Layers 6 – 8. The blue and green trend lines are water cut profiles obtained from reservoir models perforated in Layers 5 –7 and 8 –10, respectively. Cascaded on the blue and green trend lines are the neural network predictions.

The neural network model predictions were very good, especially for Reservoir (A) perforated in Layers 8 – 10 with a regression coefficient of 0.9998 and a mean square error of 1.2056e-04. The neural network model prediction for prod 2 in Reservoir (B) perforated in Layers 5 – 7 was good, but the model slightly underpredicted water cut after about 20yrs of production. The regression coefficient for this prediction is 0.9998, and the mean square error is 2.3989e-04.

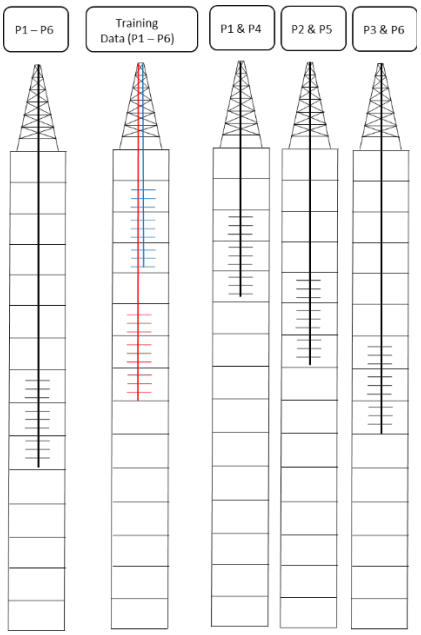


**Fig 4.7:** Schematic representation of the perforation intervals where training data were obtained and forecasting was done.

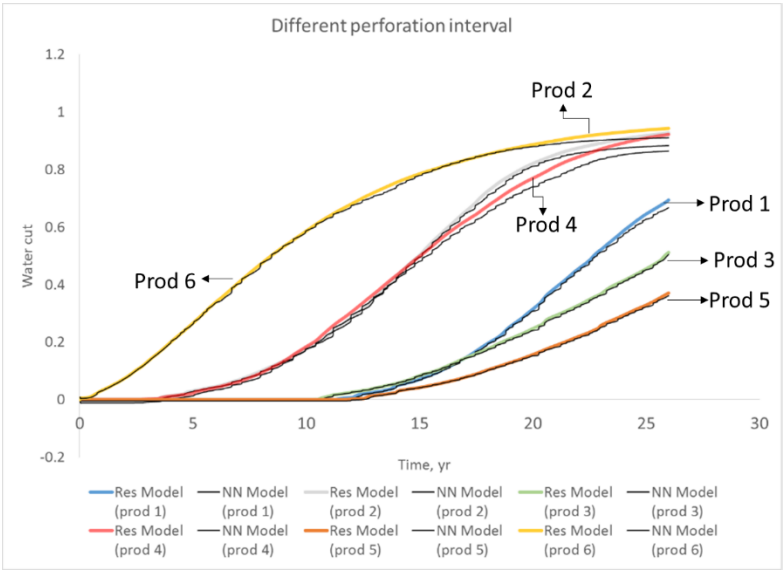


**Fig 4.8:** Water cut prediction by NET2 for all producers in a reservoir with different perforation intervals

Figure 4.8 shows the neural network predictions for all the wells perforated in model labelled Reservoir (B). The water cut prediction for prod 1, prod 3, and prod 5 were very close but the network slightly underpredicted the water cut for prod 2, prod 4 and prod 6 after 15 – 20 years of production.

As reservoir pressure declines to a level where the aquifer becomes active, water from the aquifer will move in the direction of the producer to maintain pressure. From Figure 3.2, Prod 2,

Prod 4 and Prod 6 are perforated at the deepest parts of the reservoir, which is close to the oil-water contact (OWC). There is a possibility that those producers perforated at the deepest parts of the reservoir started to produce water from the aquifer at that latter stage of simulation. Note the OWC movement was not taken into consideration in building the neural network model, and that could be the reason why NET2 slightly underpredicted the water cut of those producers perforated at the deepest parts of the reservoir model.

#### 4.2.5 Sensitivity of the NET2 to change in the distance between injector and producer

Five reservoir models were built by varying the separation distance between injector 3 (inj 3) and producer 5 (prod 5) using 300, 900, 1500, 2100 and 2700 ft. Training data were obtained from the two models with a separation distance between inj 3 and prod 5 of 900 and 1500 ft. NET2 was used to predict the water cut of prod 5 in reservoirs with a separation distance between inj 3 and prod 5 of 300, 2100 and 2700 ft.

Fig 4.10 shows the water cut profile for producers placed 300, 900, 1500, 2100 and 2700 ft. away from the injector (see Fig 4.9). NET2 slightly underpredicted water cut of the producer located 2700 ft. away from the injector after about 12 years of production with a regression coefficient of 0.9966 and mean square error of 0.0023. A better prediction was obtained for the producer located 2100 ft. away from the injector with a regression coefficient of 0.9999 and mean square error of 7.0332e-04.

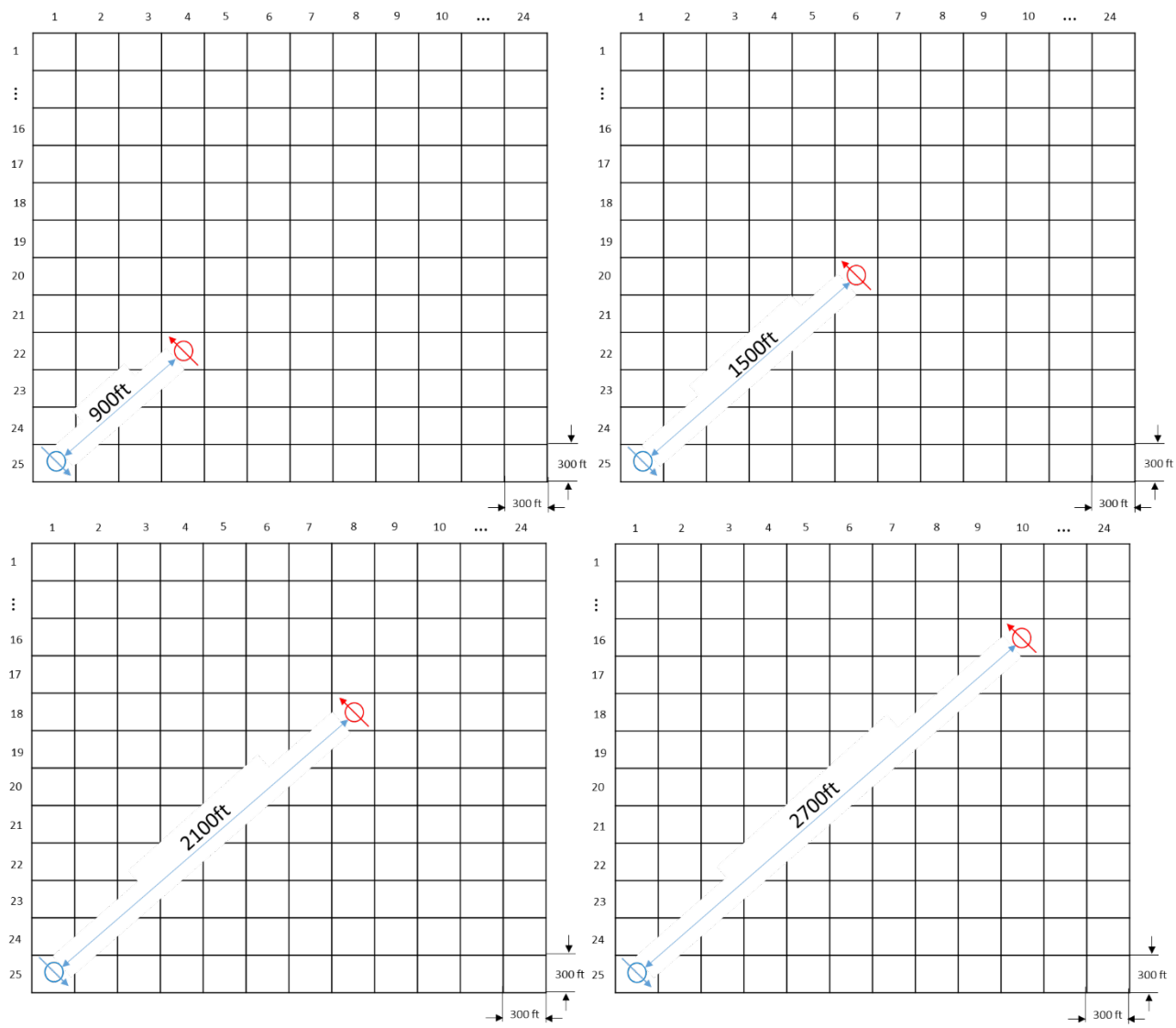


**Fig 4.9:** Schematic representation of the reservoir showing the various locations of the producers

NET2 also underpredicted the well water cut of the producer (prod 5) located 300 ft. away from the injector (inj 3) after about 2 years of production. This may be because the data set used for training the model were obtained from producers that are relatively far from the injector, and NET2 does not fully capture the impact of the 300 ft. separation between inj 3 and prod 5 on the water cut profile. The regression coefficient and mean square error with NET2's prediction of

well water cut for the producer located 300 ft. away from the injector are 0.9998 and 0.003, respectively.

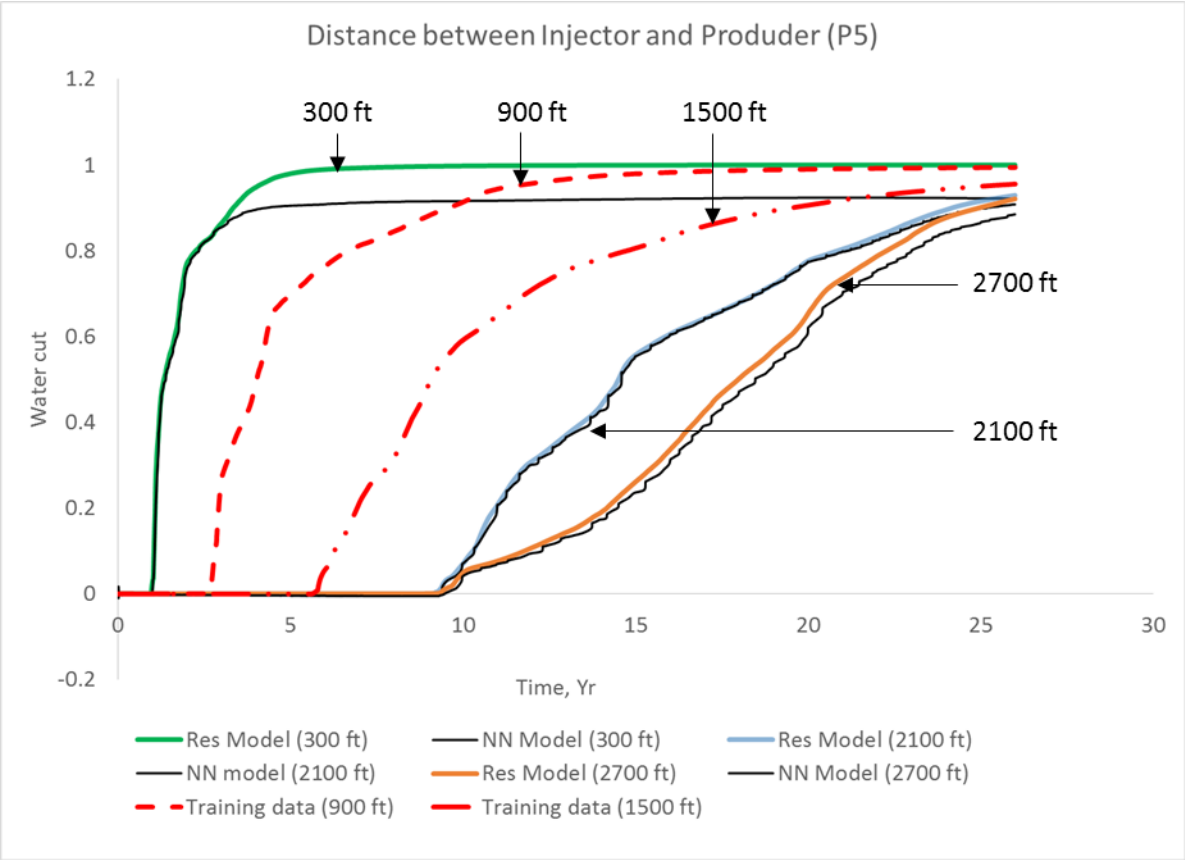


**Fig 4.10:** Water cut prediction of P5 by NET2 with changes to the separation distance between injector (Inj 3) and producer (P5)

### 4.2.6 Sensitivity of the NET2 to change in the initial aquifer pressure

Four reservoir models with initial aquifer pressure of 2000, 4000, 6000 and 8000 psi were built and simulated. The data used for training NET2 was obtained from the reservoir models with initial aquifer pressures of 2000 and 6000 psi, while the models with the initial aquifer pressures of 4000 and 8000 psi were used for prediction of water cut for the producers.

Figure 4.11 shows the results of the water cut profiles of prod 6 in all four reservoir models. NET2 was unable to accurately predict the water cut of prod 6 (P6) especially when the aquifer pressure was raised to 8000 psi. The aquifer was attached to all the cells at the base of the reservoir; this implies that pressure difference between the aquifer and the reservoir will force the movement of

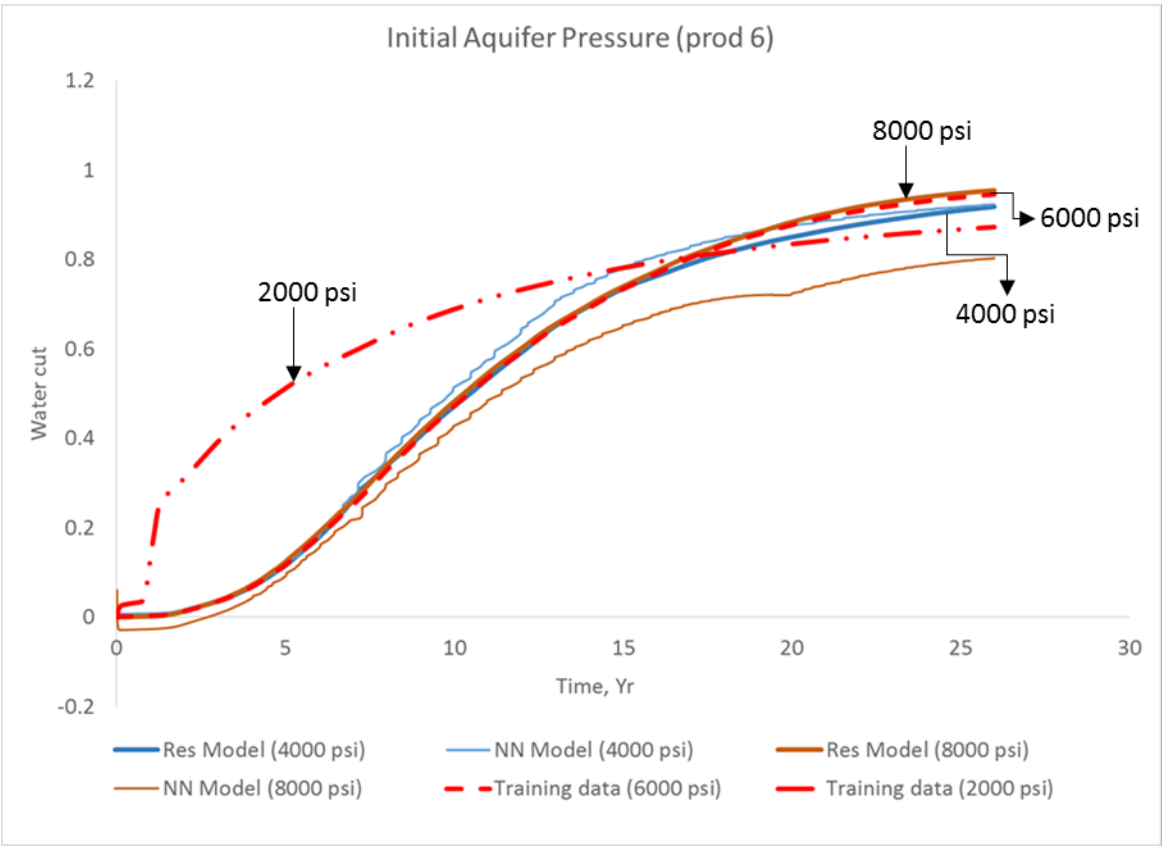


**Fig 4.11:** Water cut prediction of P5 by NET2 relative to changes in initial aquifer pressure

reservoir fluid into the wellbore, and the higher the pressure difference, the faster the movement of the OWC in the reservoir. The most likely reason for the underprediction by ANN model could be that the OWC movement considered by NET2, since training of the model did not include data describing the OWC movement. The major reason for the lack of data describing the

movement of the OWC was the difficulty in the numerical quantification of the movement of the OWC. Note, however, that Figure 4.11 shows that the well water cut prediction at Producer P6 by NET2 in the model with initial aquifer pressure of 4000 psi was better than that of the reservoir model with initial aquifer pressure of 8000 psi. The regression coefficient and mean square error obtained from the well water cut predicted at P6 in the model with initial aquifer pressure of 4000 psi are 0.9987 and $5.5020*10^{-4}$.

This data-driven approach is work in progress and presently not 100% accurate as shown in Figure 4.10, where the model underpredicted the well water cut of a producer 300ft away from an injector. However, the approach has evidently shown its predictive and forecasting capability of well water cut in a reservoir when the right data set is used in training of the neural network model. Some conclusions and recommendation have been drawn from the work so far, and they are presented in the next chapter.

# CHAPTER FIVE

## 5.0 CONCLUSIONS AND RECOMMENDATIONS

### 5.1 Summary and Conclusions

Conventional methods used to tackle the problem of excess water production in the oil and gas industry require a very good knowledge of the production mechanisms and source of water produced. The subsurface nature of the petroleum reservoir, however, makes it difficult to identify the source of water production. The artificial neural network (ANN) methodology studied in this work is a tool that can be used to predict water cut over the useful life of a reservoir without any knowledge of the source or mechanism of the produced water.

This research focused on the application of artificial neural network (ANN) to predict water cut. Some important reservoir parameters for building neural network models capable of predicting well (and field) water cut over its useful, productive life have been identified. Two neural network models were built in this study.

ANN model NET1 was used to forecast the water cut for the last 4 years of production after training the ANN model for 22 years. The input data to the ANN model consisted of 26 years of water cut production history.

To evaluate the predictive capability and robustness of the ANN methodology, a second neural network model, NET2, was developed. NET2 was used to investigate the sensitivity of ANN predicted results to changes in several reservoir properties and operational parameters. The sensitivity study included examining the effect of changes in permeability contrast, horizontal permeability, perforation interval of producers, and the separation distance between producer and injector on ANN predicted water cuts. In all the cases investigated, the results show close matches between the input data (water cut) and the ANN predicted results. The results from the

comparison between input data and ANN predicted water cuts show very high regression coefficients ($R^2 > 0.98$) and low mean square errors.

The ANN tools developed in this work have been tested, with promising results. If given proper attention, the application of artificial neural network tools could someday become significant players in tackling the problem of excess water production in the oil and gas industry.

## 5.2 Recommendations

Further research work on the application of artificial neural network for solving excess water production problem in the oil and gas industry should consider some of the following points.

First, the major problem with Chan's (1995) log-log plot of the water-oil ratio (WOR) and WOR derivative against time is that it only works well when simulated production data is used. When real field production data is used, the noisy nature of the field data makes the supposed diagnostic signatures of different mechanisms of excess water production indistinguishable. Hence future research should target the development of robust neural network models with real field production data to solve the problem of excess water production in the oil and gas industry.

Second, future research should investigate a way to accurately track the movement of the oil-water contact (OWC). This will enable the incorporation of data describing the OWC movement and the dynamics of the reservoir behaviour into the training data sets used in artificial neural network modelling. This will further improve the predictive capabilities of the neural network models used to solve the problem of excess water production.

Finally, it is recommended that multilayer neural networks other than NARXNET used in this work be considered for future research.

## REFERENCES


1. Al-Bulushi, N., Araujo, M., Kraaijveld, M., & Jing, X. D. (2007). Predicting water saturation using artificial neural networks (ANNS). In *SPWLA Middle East Regional Symposium*. Society of Petrophysicists and Well-Log Analysts.
2. Al-Ghanim, J. A., & Al-Nufaili, S. A. (2010, January). Middle East Field Water Production Mechanisms. In SPE Oil and Gas India Conference and Exhibition. Society of Petroleum Engineers
3. Al Hasani, M. A., Khayari, A., Rashid, S., Al Maamari, R., & Al-Wadhahi, M. A. (2008, January). Diagnosis of excessive water production in horizontal wells using WOR plots. In International Petroleum Technology Conference. International Petroleum Technology Conference.
4. Alghazal, M. (2015). Development and Testing of Artificial Neural Network Based Models for Water Flooding and Polymer Gel Flooding in Naturally Fractured Reservoirs.
5. Arnold, R., Burnett, D. B., Elphick, J., Feeley, T. J. I. I. I., Galbrun, M., Hightower, M., & Verbeek, P. (2004). Managing water–from waste to resource. *Oilfield Review*, *16*(2), 26-41.
6. Bailey, B., Crabtree, M., Tyrie, J., Elphick, J., Kuchuk, F., Romano, C., & Roodhart, L. (2000). Water control. *Oilfield Review*, *12*(1), 30-51.
7. Beale, M. H., Hagan, M. T., & Demuth, H. B. (2017). Neural network toolbox™ user's guide. In *R2017a, The MathWorks, Inc., 3 Apple Hill Drive Natick, MA 01760-2098, www. mathworks.com*.
8. Boyun, G., William, C., & Ali Ghalambor, G. (2007). *Petroleum production engineering: a computer-assisted approach*. Elsevier Science & Technology Books.
9. BuKhamseen, N. (2014). *Applications of Artificial Expert Systems in the Diagnosis and Analysis of Unexpected Spatial and Temporal Changes in Reservoir Production*

*Behavior*. The Pennsylvania State University. Demuth, H. B., Beale, M. H., De Jess, O., & Hagan, M. T. (2014). *Neural network design*. Martin Hagan.

10. Chan, K. S. (1995, January). Water control diagnostic plots. In SPE Annual Technical Conference and Exhibition. Society of Petroleum Engineers.
11. Demuth, H. B., Beale, M. H., De Jess, O., & Hagan, M. T. (2014). *Neural network design*. Martin Hagan.
12. Egbe, T., & Appah, D. (2005, January). Water Coning Diagnosis Using Spectral Analysis. In Nigeria Annual International Conference and Exhibition. Society of Petroleum Engineers.
13. Ershaghi, I., Handy, L. L., & Hamdi, M. (1987). Application of the x-Plot Technique to the Study of Water Influx in the Sidi El-Itayem Reservoir, Tunisia (includes associated paper 17548). Journal of Petroleum Technology, 39(09), 1-127.
14. Fausett, L. (1994). *Fundamentals of neural networks: architectures, algorithms, and applications* (No. 006.3). Prentice-Hall.
15. Hegeman, P. S., Dong, C., Varotsis, N., & Gaganis, V. (2009). Application of artificial neural networks to downhole fluid analysis. *SPE Reservoir Evaluation & Engineering*, *12*(01), 8-13.
16. Killough, J. E. (1995, January 1). Ninth SPE Comparative Solution Project: A Reexamination of Black-Oil Simulation. Society of Petroleum Engineers. doi:10.2118/29110-MS
17. Maren, A. J., Harston, C. T., & Pap, R. M. (2014). *Handbook of neural computing applications*. Academic Press.
18. Maurya, A. K., Mahto, V., Sharma, V. P., & Laik, S. (2014). Study of the Potential of Amino Resin to Control Excessive Water Production in the Indian Oilfields. *Petroleum Science and Technology*, *32*(12), 1443-1447. http://dx.doi.org/10.1080/10916466.2012.685542
19. McCulloch, W. S., & Pitts, W. (1943). A logical calculus of the ideas immanent in nervous activity. *The bulletin of mathematical biophysics*, *5*(4), 115-133.

20. Nakutnyy, P., Asghari, K., & Torn, A. (2008). Analysis of waterflooding through application of neural networks. In *Canadian International Petroleum Conference*. Petroleum Society of Canada.
21. Njoku, C., Horst, P., & Akinsanmi, O. (2013). Application of Neural Network Workflow to Facies Modeling in Turbidite Reservoirs, Offshore Nigeria. In *SPE Nigeria Annual International Conference and Exhibition*. Society of Petroleum Engineers.
22. Novotny, R. J. (1995, January). Matrix flow evaluation technique for water control applications. In SPE European Formation Damage Conference. Society of Petroleum Engineers.
23. Panda, M. N., Zaucha, D. E., Perez, G., & Chopra, A. K. (1996). Application of neural networks to modeling fluid contacts in Prudhoe Bay. *SPE Journal*, *1*(03), 303-312.
24. Parada, C. H. (2008). *An Artificial Neural Network Based Tool-Box for Screening and Designing Improved Oil Recovery Methods* (Doctoral dissertation, Ph. D. dissertation, The Pennsylvania State University, University Park, Pennsylvania).
25. Renpu, W. (2011). Advanced well completion engineering. Gulf Professional Publishing.
26. Reynolds, R. R., & Kiker, R. D. (2003). Produced Water and Associated Issues. *Oklahoma Geological Survey*.
27. Rosenblatt, F. (1958). The perceptron: A probabilistic model for information storage and organization in the brain. *Psychological review*, *65*(6), 386.
28. Saeedi, A., Camarda, K. V., & Liang, J. T. (2007). Using neural networks for candidate selection and well performance prediction in water-shutoff treatments using polymer gels-a field-case study. *SPE Production & Operations*, *22*(04), 417-424.
29. Schlumberger, (2017). Eclipse Reference Manual.
30. Seright, R. S. (1998). Improved methods for water shutoff. *Final Technical Progress Report (US DOE Report DOE/PC/91008-14), US DOE Contract DE-AC22-94PC91008, BDM-Oklahoma Subcontract G4S60330 (Oct. 1998)*, 21-54.
31. Seright, R. S., Lane, R. H., & Sydansk, R. D. (2003). A strategy for attacking excess water production. In *SPE Permian Basin Oil and Gas Recovery Conference*. Society of Petroleum Engineers.

32. Sunday, A. C. (June, 2016). Artificial neural network for diagnosis and mitigation of water production. MSc Thesis, African University of Science and Technology, Abuja, Nigeria.
33. Yortsos, Y. C., Choi, Y., Yang, Z., & Shah, P. C. (1997, January). Analysis and interpretation of the water-oil ratio in waterfloods. In SPE Annual Technical Conference and Exhibition. Society of Petroleum Engineers.

## APPENDIX A

**Appendix A-1:** Input parameter to ANN Models, NET1 and NET2

**Table A.1:** Neural network input parameters

| S/n | Parameter | Unit | Symbol | Source |
|---|---|---|---|---|
| 1 | Well water production rate | bbl/day | WWPR | Producers |
| 2 | Well productivity index | bbl/day/psi | WPI | |
| 3 | Well oil production rate | bbl/day | WOPR | |
| 4 | Well gas production rate | MMscf/day | WGPR | |
| 5 | Well gas – oil ratio | | WGOR | |
| 6 | Well bottom hole pressure | psi | WBHP | |
| 7 | Pressure of the last perforation block | psi | PBLK | |
| 8 | Well water injection rate of injector 1 | bbl/day | WWIR: Inj1 | Injectors |
| 9 | Well water injection rate of injector 2 | bbl/day | WWIR: Inj2 | |
| 10 | Well water injection rate of injector 3 | bbl/day | WWIR: Inj3 | |
| 11 | Well water injection rate of injector 4 | bbl/day | WWIR: Inj4 | |
| 12 | Field pressure | psi | FPR | Field |
| 13 | Separation distance between inj 3 and prod 5 | Ft | SD | Field |
| 14 | Porosity of the first perforated layer | | $\phi(1)$ | Perforated layers |
| 15 | Porosity of the second perforated layer | | $\phi(2)$ | |
| 16 | Porosity of the third perforated layer | | $\phi(3)$ | |
| 17 | Permeability contrast | | $K_v/k_h$ | |
| 18 | Horizontal permeability | md | $K_h$ | |
| 19 | Perforation tops | Ft | PT | |
| 20 | Thickness of the first perforated layer | ft. | DZ(2) | |
| 21 | Thickness of the second perforated layer | ft. | DZ(3) | |
| 22 | Thickness of the third perforated layer | ft. | DZ(4) | |
| 23 | Aquifer length | ft. | AL | Aquifer |
| 24 | Aquifer pressure | psi | AP | |
| 25 | Distance between aquifer and perforation zone | Ft | DAP | Field |

**Table A.2:** Reservoir conditions for the base and modified model

| S/n | Symbol | Base model parameter | Modified model parameter | Source |
|---|---|---|---|---|
| 1 | WWPR | Simulation result | Simulation result | Producers |
| 2 | WPI | Simulation result | Simulation result | |
| 3 | WOPR | Simulation result | Simulation result | |
| 4 | WGPR | Simulation result | Simulation result | |
| 5 | WGOR | Simulation result | Simulation result | |
| 6 | WBHP | Simulation result | Simulation result | |
| 7 | PBLK | Simulation result | Simulation result | |
| 8 | WWIR: Inj1 | 0 psi | Pressure | |

| | | | | |
|---|---|---|---|---|
| 9 | WWIR: Inj2 | 0 psi | maintenance (6000 psi) | Injectors |
| 10 | WWIR: Inj3 | 0 psi | | |
| 11 | WWIR: Inj4 | 0 psi | | |
| 12 | FPR (Datum) | 5000 psi | 5000 psi | Field |
| 13 | SD | 1500 ft. | 300 – 2700 ft. | Field |
| 14 | $\phi(1)$ | 0.097 | Varies depending on the perforation interval | Perforated layers |
| 15 | $\phi(2)$ | 0.111 | | |
| 16 | $\phi(3)$ | 0.16 | | |
| 17 | $K_v/k_h$ | 0.1 | 0.01 - 1 | |
| 18 | $K_h$ | 108.1 md | 400 – 1200 md | |
| 19 | PT (P1) | 9337.39 ft. | Calculated | |
| 20 | DZ(2) | 15 ft. | Varies depending on the perforation interval | |
| 21 | DZ(3) | 26 ft. | | |
| 22 | DZ(4) | 15 ft. | | |
| 23 | AL | 718 ft. | 718 ft. | Aquifer |
| 24 | AP | 6000 psi | 0 - 6000 psi | |
| 25 | DAP (P1) | 923.27 ft. | Calculated | Field |